DETERMINATION OF THE MOST SUITABLE WAVELENGTH INTERVALS FOR OPTICAL DATA TRANSMISSION THROUGH THE ATMOSPHERE

A THESIS SUBMITTED TO
THE GRADUATE SCHOOL OF NATURAL AND APPLIED SCIENCES
OF
MIDDLE EAST TECHNICAL UNIVERSITY

BY

YÜCEL CENGİZ ÖZER

IN PARTIAL FULFILLMENT OF THE REQUIREMENTS
FOR
THE DEGREE OF MASTER OF SCIENCE
IN
PHYSICS

SEPTEMBER 2006

Approval of the Graduate School of Natural and Applied Sciences

Prof. Dr. Canan Özgen
Director

I certify that this thesis satisfies all the requirements as a thesis for the degree of Master of Science.

Prof. Dr. Sinan Bilikmen
Head of Department

This is to certify that we have read this thesis and that in our opinion it is fully adequate, in scope and quality, as a thesis for the degree of Master of Science.

Assoc.Prof. Dr.Akif Esendemir
Supervisor

Examining Committee Members

Prof. Dr. İbrahim GÜNAL (METU, PHYS) _____

Assoc. Prof. Dr. Akif ESENDEMİR (METU, PHYS) _____

Assoc. Prof. Dr. Enver BULUR (METU, PHYS) _____

Assoc. Prof. Dr. Serhat ÇAKIR (METU, PHYS) _____

Dr. Ali ALAÇAKIR (TAEK, SANAEM) _____

I hereby declare that all information in this document has been obtained and presented in accordance with academic rules and ethical conduct. I also declare that, as required by these rules and conduct, I have fully cited and referenced all material and results that are not original to this work.

Name, Last name : Yücel Cengiz, ÖZER

Signature :

ABSTRACT

DETERMINATION OF THE MOST SUITABLE WAVELENGTH INTERVALS FOR OPTICAL DATA TRANSMISSION THROUGH THE ATMOSPHERE

Özer, Yücel Cengiz
M.S., Department of Physics
Supervisor: Assoc. Prof. Dr.Akif Esendemir

September 2006, 60 pages

Optical Wireless Communication systems use lasers offering larger bandwidth, which facilitates higher data rates, comparing with radio communication systems. However, its performance is limited by atmospheric conditions, and is a function of wavelength.

The objective of this study is the determination of the wavelength interval(s) at which the atmospheric transmittance is relatively high and has relatively low dependence on variations in temperature, relative humidity, wind speed and atmospheric pressure under the conditions such as path altitude of 10 meters, path geometry of horizontal to the Earth's surface and clean (includes no fog, rain or snow etc.) over sea surface atmosphere. The path length is taken to be 15 km.

Alanya was assignated as geographical region and the required information about the atmospheric constituents and meteorological parameters was collected. Then, the variations in atmospheric transmittance due to the periodically measured

meteorological parameters were calculated (for summer and winter seasons). Finally, individually calculated effects of these parameters on atmospheric transmittance are assembled in order to determine the desired wavelength interval(s). As a result, the most suitable wavelength interval was determined to be about between 3.99 μm and 4.02 μm.

In addition, dependencies of atmospheric pressure, temperature, relative humidity, and wind speed on atmospheric transmittance have been established for both winter and summer seasons. Atmospheric transmittance is found to be inversely proportional to temperature, relative humidity and wind speed. The effect of pressure is relatively small comparing with other parameters.

Keywords : Atmospheric Transmittance, Transmission, Optical Wireless Communication, Wavelength Selection

ÖZ

ATMOSFERDEN OPTİK VERİ İLETİŞİMİ İÇİN
EN UYGUN DALGA BOYU ARALIKLARININ BELİRLENMESİ

Özer, Yücel Cengiz
Yüksek Lisans, Fizik Bölümü
Tez Yöneticisi: Doç. Dr. Akif Esendemir

Eylül 2006, 60 sayfa

Kablosuz Optik İletişim sistemleri, lazer kullandıklarından dolayı, radyo frekans iletişim sistemlerine göre daha yüksek bant genişliği, dolayısiyle daha yüksek veri iletişim hızları öngörmektedir. Sistem performansı atmosfer koşulları ile sınırlanmakta ve dalga boyuyla değişkenlik göstermektedir.

Bu çalışmanın konusu, temiz (sis, yağmur, kar vs. içermeyen), deniz yüzeyi atmosferinde, 10 m yükseklikte yüzeye paralel bir menzil için, atmosferik geçirgenliğin, sıcaklık, bağıl nem, rüzgar hızı ve atmosferik basınç değişimlerinden mümkün olduğunca az etkilenen, ve atmosferik geçirgenliğin mümkün olduğunca yüksek olduğu dalga boyu aralığı/aralıklarının belirlenmesidir. Çalışmada menzil 15 km olarak alınmıştır.

Coğrafi konum olarak Alanya belirlenmiştir ve bu bölge için, atmosferik içerik bilgisi ve meteorolojik parametreler toplanmıştır. Daha sonra, periyodik olarak

ölçümü yapılan meteorolojik parametrelerin, atmosferik geçirgenlik üzerinde ne gibi değişimlere sebep olduğunun hesaplamaları yapılmıştır (yaz ve kış mevsimleri için). Son olarak da, her bir meteorolojik parametrenin atmosferik geçirgenlik üzerindeki hesaplanan etkileri bir araya getirilerek, bulunmak istenen dalga boyu aralığı saptanmıştır. Sonuç olarak, dalga boyu aralığı yaklaşık 3.99 - 4.02 μm olarak belirlenmiştir.

Buna ilaveten, atmosferik geçirgenliğin, sıcaklık, atmosferik basınç, bağıl nem ve rüzgar hızındaki değişimlerin etkisine bağımlılığı, hem kış hem de yaz mevsimi için saptanmıştır. Atmosferik geçirgenlik, sıcaklık, bağıl nem ve rüzgar hızı ile ters orantılıdır. Basıncın etkisinin, diğer parametrelere oranlara nispeten çok daha az olduğu görülmüştür.

Anahtar kelimeler : Atmosferik Geçirgenlik, Kablosuz Optik İletişim,
Dalgaboyu Seçimi

To My Mother

and

Living Memory of My Father

ACKNOWLEDGMENTS

I would like to thank my supervisor Assoc. Prof. Dr. Akif Esendemir for his valuable guidance, suggestions and kind interest regarding my thesis.

Special thanks go to Prof. Dr. Gürdal Tuncel, Prof. Dr. Yurdanur Tulunay and Prof. Dr. Şahinde Demirci because of their advice, support and help.

I would like to express my gratitude to my dear friend Esen Salçın for her encouragement, help, support, and friendship.

Special thanks also go to my friends, Selçuk Yerci, Nader Ghazanfari, Sami Kama, and İlker Kılıç who always shared my excitements and enthusiasms during my study.

It is a very big pleasure for me to thank to my family, without their valuable support, all this work would not be possible.

TABLE OF CONTENTS

LIST OF FIGURES

FIGURE

LIST OF TABLES

TABLE

LIST OF ABBREVIATIONS

AFCRL:	Air Force Cambridge Research Laboratories
AFGL:	Air Force Geophysics Laboratory
AT:	Atmospheric Transmittance
FSO:	Free-Space Optics
HITRAN:	HIgh-Resolution TRANsmission Molecular Absorption Database
MLS:	Mid Latitude Summer
MLW:	Mid Latitude Winter
MODTRAN:	MODerate Resolution TRANsmittance Code
NAM:	Navy Maritime Aerosol Model
OWC:	Optical Wireless Communication
ppmv:	Parts Per Million By Volume
UV:	Ultra-Violet

CHAPTER 1

INTRODUCTION

There is an increasing demand on laser involved applications due to the unique features of laser light (i.e. monochromatic, unidirectional, coherent etc.). One of the important applications is Optical Wireless Communication (OWC), or Free-Space Optics (FSO). It is a system that works in optical frequencies (from UV throughout infrared) that have enormous potential for data transmission; offering large bandwidth, which facilitates higher data rates comparing with radio frequencies [1] [2]. OWC systems are used for a variety of applications [2] in order to communicate between ground, air, space, and naval platforms [3]. A schematical representation of an OWC system is shown in Figure 1.1 [2].

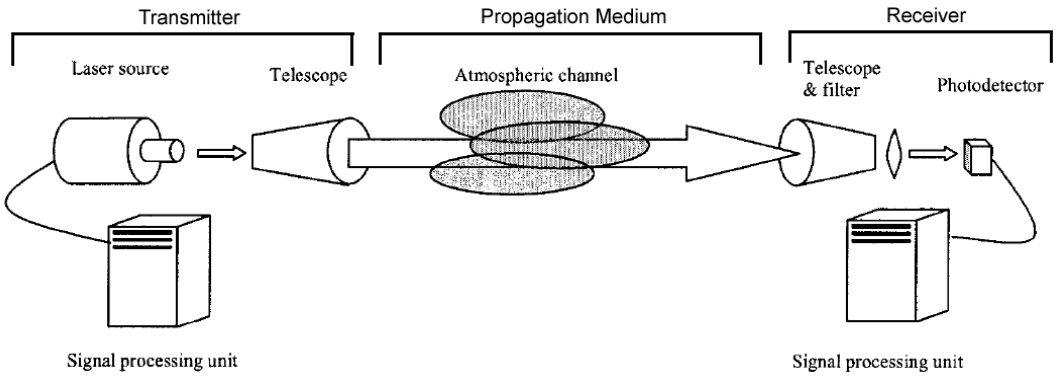

Figure 1.1. Schematical representation of a basic Optical Wireless Communication System (Adopted from [2]).

An OWC system, like other electro-optical systems, consists of three basic components: a transmitter, a propagation medium, and a receiver (includes optical systems and detectors). For propagation medium that can not be intervened, the selection and design of source, detector, and optical systems are mainly limited with the characteristics of the propagation medium. Because of the convenient quality of source and detector systems today, atmosphere is such a medium that is often the deterministic factor in overall system design and performance [4]. Therefore, a throughout discussion about atmospheric effects on optical propagation of radiation is required for proper system design issues.

One of the most critical parameters for predicting the system performance is the *atmospheric transmittance* (AT) that describes the decrease in intensity of propagating radiance. This decrease in intensity is due to the interaction of photons with the atmospheric constituents. Since the atmospheric composition and its physical state (i.e. temperature and pressure) are highly variable with respect to geographical location, altitude and time, enormous variations can be observed in AT.

The change in atmospheric transmittance is not the same for all the wavelengths. Thus, the performance of OWC and other electro-optical systems depend on the operation wavelength [5]. In order to explore suitable wavelengths, various AT studies depending on different meteorological conditions have been done previously [2]. Nowadays, OWC systems usually operate in near-IR; however, various studies indicate that weather effects can be minimized by use of medium-IR and far-IR sources [2].

Meteorological observations show that basic meteorological parameters, such as temperature, relative humidity, and wind speed are highly variable with time [6]. Along with atmospheric pressure, these parameters affect AT [7-9]. By taking these considerations into account, aim of this study is to determine specific wavelength intervals(s) at which the effect of meteorological parameters (i.e. pressure,

temperature, relative humidity, and wind speed) on AT is relatively low and the AT is relatively high. For the study, the range of wavelengths, 0.3-14 μm have been scanned throughout the work under the following conditions:

- Horizontal path over sea surface,
- Path length of 15 km,
- Path altitude of 10 meters,
- Clean atmosphere (includes no fog, rain, or snow etc.),
- Geographical location is Alanya region (located at the south coast of Turkey, at the coastal zone of Eastern Mediterranean).

In Chapter 2, the structure and composition of the atmosphere is given. The AT is described, and interaction of photons with atmospheric constituents is explained. The criteria of selection of geographical location, and the required information about the atmospheric constituents are presented in Chapter 3. Then, the calculated variations in AT due to the periodically measured meteorological parameters and their results are given. As a final step, individual effects of the meteorological parameters on AT are gathered in order to determine the desired wavelength interval(s). In Chapter 4, the conclusion of the study, overall evaluation of the results is given.

CHAPTER 2

OPTICAL ATMOSPHERIC TRANSMISSION

The optical nature of the atmosphere involves emission, absorption, scattering, reflection, and refraction of radiation. Any incoming radiation interacts with the atmospheric constituents, which under normal conditions, are various gaseous species and small particles [10]. The power of incident radiance reduces while propagating through the atmosphere due to absorption and scattering by gaseous molecules and particles. The fraction of incident radiance intensity that reaches to a specific range is defined as *atmospheric transmittance* [11].

In this chapter, atmospheric transmittance is covered; however, it depends on atmospheric constituents and their physical states (i.e. temperature). Therefore, first, understanding the atmospheric environment is necessary.

2.1. Atmospheric Environment

The atmosphere is a highly inhomogeneous fluid composed of gases and suspended particles at various temperatures and pressures. Their physical and chemical properties vary as a function of time, altitude and geographical location [10] [4]. Thus, determining the optical properties of the atmosphere requires understanding the structure of the atmosphere and its composition [12]. Specifically, in order to model the atmospheric transmittance and radiance, the requirements are: molecular concentrations, particle concentrations, particle characteristics (i.e. size, shape, and

chemical composition), and the physical state of the atmosphere (i.e. pressure and temperature).

2.1.1. Atmospheric Structure

Gravity holds the atmosphere to the Earth's surface and it slowly becomes thinner and fades away with increasing altitude into space extending out many thousands of kilometers from the surface of the Earth [13]. It does not technically end at any given height. However, an altitude of 120 km marks the boundary where atmospheric effects become considerable [14]. The Karman line (at 100 km) is also frequently used as the boundary between atmosphere and space [15].

Below 120 km altitude, four main horizontal layers form the stratified structure of the atmosphere; *troposphere*, *stratosphere*, *mesosphere*, and *thermosphere*. These distinct layers have been determined by using thermal characteristics, chemical composition, movement, and density of atmosphere. They are bounded by "pauses" (Figure 2.1) where the maximum changes occur [16]. The layers along with temperature and pressure profiles representing two seasonal (summer and winter) standard atmospheres for typical mid latitude (45N) conditions, are shown in Figures 2.1 and 2.2.

The atmospheric *pressure* can be related to the weight of the air over a specific location, and is generally measured in millibars (1 mbar = 1 g/cm^2). Other units are kilo-pascals (kPa), torr (mm Hg), and atmospheres (atm), where 1atm = 1013 mbar = 101.3 kPa = 760 torr. The pressure decreases exponentially with increasing altitude [4] (Figure 2.1). Since the amount (or weight) of air above the earth varies with location and time, pressure varies similarly [14]. At sea level, pressure ranges from about 960 to 1050 mbar with an average of 1013 mbar [18].

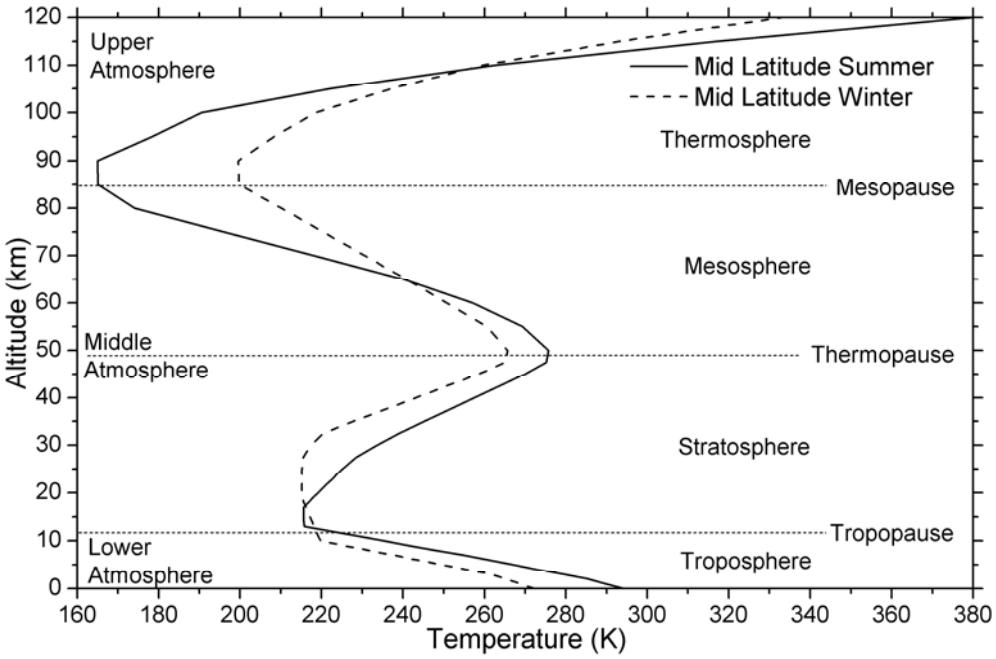

Figure 2.1. Atmospheric layers, and vertical temperature profiles for mid latitude summer and winter seasons (Adopted from [17] and [12]).

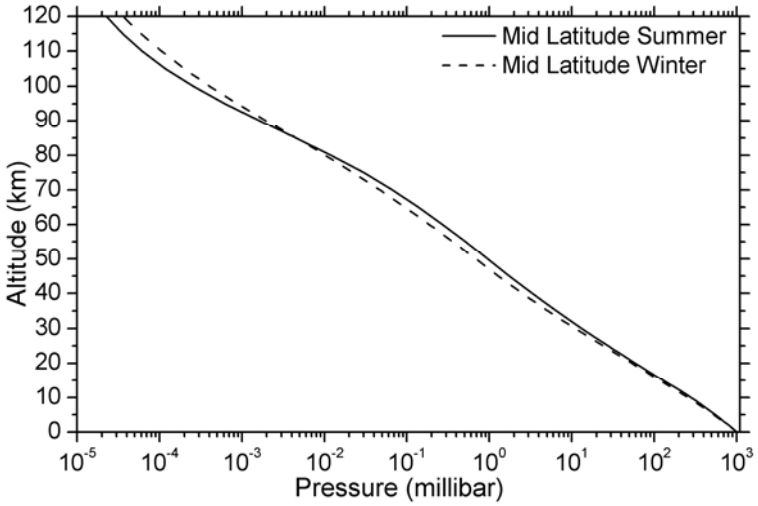

Figure 2.2. Vertical pressure profiles for mid latitude summer and winter seasons (Adopted from [17]).

The lowest layer, *troposphere* begins at the Earth's surface and extends up to 6-20 km high [16]. The height of the upper boundary tropopause varies from the equator (around 18-20 km) to the poles (just under 6.5 km). The tropopause and the troposphere are known as the *lower atmosphere* [16] that contains about half of the Earth's atmosphere [19]. The temperature varies frequently, and decreases linearly from a mean surface temperature of about 288 K to a temperature of about 220 K at a rate of 6.5 K/km^{-1} [4] [12]. Almost all weather occurs in this region; clouds and fog form, precipitation falls, wind blows, humidity varies from place to place, and the atmosphere interacts with the surface of the earth below [18] [16]. Most of the important atmospheric attenuators exist in this layer (i.e. water vapor, carbon dioxide, clouds, fog, and aerosols in general) [4]. In the *boundary layer* (surface to 1-2 km altitude [10]), the atmospheric interaction with the surface is strong and significant. Thus, the troposphere, especially the boundary layer, has a major importance in optical atmospheric phenomenon [12].

The *stratosphere* extends from the tropopause up to 48 km above the Earth's surface. This layer holds about 19 percent of the atmospheric gases. Ozone layer or ozonosphere is located in this layer and extends approximately 10 to 50 km [14]. The temperature increases from tropopause to the stratopause (about 270 K). The absorption of sun fluxes (ultraviolet) by ozone and through the emission of infrared fluxes by carbon dioxide determines the state of the stratosphere [12]. The increasing temperature also makes it a calm layer. The movements of the gases are slow [16]. The stable character of the stratosphere yields persisting of thin layers of aerosols for a long time within certain altitudes [12].

The *mesosphere* extends from the stratopause to about 85-90 km above the surface of the Earth. The effect of the warming by ultraviolet radiation becomes less, leading to a decrease in temperature from about -15°C to as low as -120°C at the mesopause [16] [4]. The mesosphere and the stratosphere are known as *middle atmosphere* [12].

The *thermosphere*, known as the *upper atmosphere*, extends from the mesopause to 690 km above the Earth's surface. The gases in the thermosphere are increasingly thinner than in the mesosphere. Only the higher energy ultraviolet and x-ray radiation from the sun are absorbed [16]. Located within the thermosphere, the ionosphere (60 - 300 km) is made of electrically charged gas particles (ionized plasma) [20]. It is important for radio-wave propagation because of the reflective characteristics; however, this layer is optically transparent. The optical atmospheric radiation and transmittance modeling generally end up with mesosphere [4].

2.1.2. Gaseous Composition of Atmosphere

The Earth's atmosphere consists of various gases. The variability in abundances of these gases with altitude and time do not show same characteristics. Table 2.1 lists uniformly mixed atmospheric gases (up to 100km) and their abundances for a dry atmosphere (i.e. no moisture included).

Table 2.1. Gaseous composition of the atmosphere (uniformly mixed gases) [4].

Constituent	***Volume Ratio (%)***	***Parts Per Million by Volume (ppmv)***
Nitrogen, N_2	78.084 ± 0.004	-
Oxygen, O_2	20.946 ± 0.002	-
Argon, Ar	0.934 ± 0.001	-
Neon, Ne	0.001818	18.18 ± 0.04
Helium, He	$5.24 * 10^{-4}$	5.24 ± 0.004
Krypton, Kr	$1.14 * 10^{-4}$	1.14 ± 0.01
Xenon, Xe	-	0.087 ± 0.001
Hydrogen, H_2	-	0.5
Methane, CH_4	-	1.6
Nitrous oxide, N_2O*	-	0.5 ± 0.1
***Has varying concentration in polluted air.		

Gases listed in Table 2.1 do not vary significantly in concentration with time. They have basically fixed relative concentrations with differing altitude. Generally, the inert gases contribute little to optical atmospheric phenomena [4].

Oxygen and nitrogen are by far the most abundant gases; however, they contribute little to opacity. They are important for molecular scattering phenomenon (see section 2.5.2) [4].

Some of the most important infrared active molecules have variable concentration. These molecules are listed in Table 2.2 including H_2O, CO_2 and O_3.

Table 2.2. Gaseous composition of the atmosphere (present in variable amounts)[4].

Constituent	***Volume Ratio (%)***	***Parts Per Million by Volume (ppmv)***
Ozone, O_3	- -	0 – 0.3 (tropospheric*) 1 – 7 (20 to 30 km)
Water vapor, H_2O	0 – 2	-
Carbon dioxide, CO_2	0.035	351 ± 4
Carbon monoxide, CO*	-	0.19
Nitric acid vapor, HNO_3	-	(0 to 10) * 10^{-3}
Ammonia, NH_3	-	Trace
Hydrogen sulfide, H_2S	-	(2 to 20) * 10^{-3}
Sulfur dioxide, SO_2*	-	(0 to 20) * 10^{-3}
Nitrogen dioxide, NO_2	-	Trace
Nitric oxide, NO	-	Trace
***Has varying concentration in polluted air.		

The abundances of variable gases are small; however, they are extremely important in optical atmospheric phenomena. Water vapor is the major radiatively active molecule in the Earth's atmosphere. Its variability in concentration is significant in geographical location, altitude, and time [12].

Figure 2.3 shows altitude dependent concentrations of some important molecules for typical mid latitude conditions.

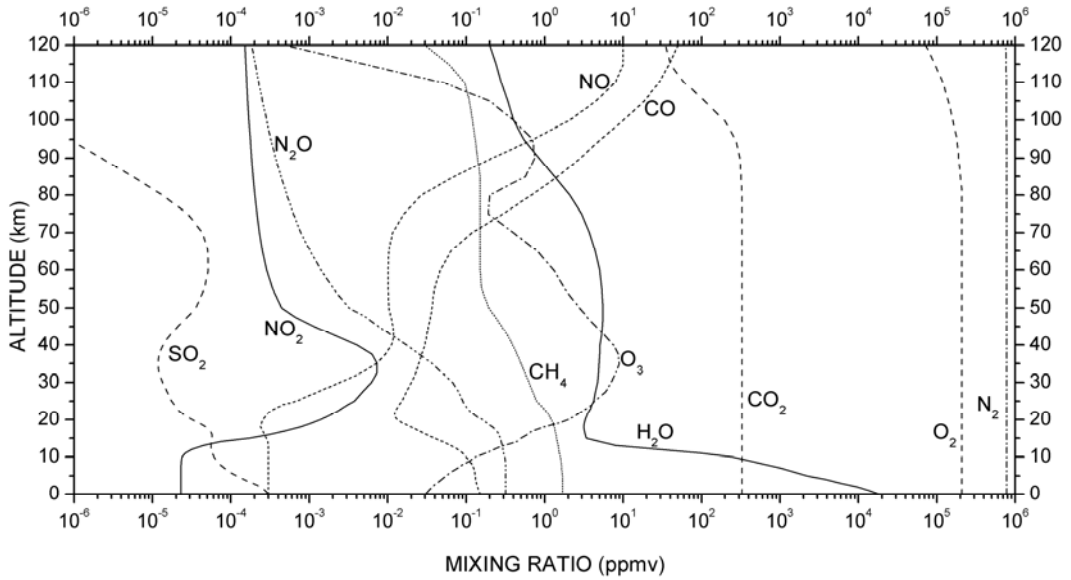

Figure 2.3. Vertical profiles of mixing ratios of some important atmospheric gases (Mid Latitude Summer atmospheric constituent profile) [17].

Relative humidity (see Appendix A) rapidly decreases with pressure (almost follow an exponential function). More than 90% of water vapor confined to the altitude below ~500 mbar. Humidity also decreases with latitude [12].

Carbon dioxide is uniformly mixed with altitude up to about 80 km, and varies seasonally with a maximum during the early spring and a minimum during the late summer to early fall [4]. Its abundance increases with an annual average of 0.4% per year as a result of photosynthesis, fossil fuels, absorption and release by the oceans [12].

Methane concentration has been increasing by 1-2% by volume per year due to rice paddies, and greater biogenic emission with the rising human population [12].

Carbon monoxide concentration increases with deforestation, biomass burning, and modification of CH_4 sources [12]. Because of the combustion of fossil fuels, the abundance of nitrous oxide increases at a rate of about 0.2% per year [12].

Ozone concentration varies significantly with geographical location and time. However, ozone is primarily concentrated at altitudes from ~15 to 30 km, namely at ozone layer [12]. Its concentration is relatively low in the boundary layer [4].

In the stratosphere, volcanic eruptions yield large amounts of sulfur dioxide which is responsible for forming the primary stratospheric aerosols [12].

2.1.3. Atmospheric Constituent Profiles

There are some technical difficulties in measuring some gas concentrations, density, temperature, and pressure of the atmosphere up to altitudes of 120 km. There are many atmospheric constituents profile databases in literature which may be used for case study. One widely used realistic database is that of compiled by AFGL (Air Force Geophysics Laboratory) [17]. This database has been designed for incorporation into atmospheric radiation modeling, and consists of realistic vertical (0-120 km) profiles for temperature, pressure, density, and gas mixing ratios allowing a wide range of climatological choices and geographical location. Its thermal structure is represented by tropical (15N latitude), middle latitude (45N latitude) summer (MLS) and winter (MLW), sub arctic (60N latitude) summer and winter, and the U.S. standard model atmosphere, 1976 [17]. These are known to be six reference atmospheres. Temperature and pressure profiles for MLS and MLW are shown in Figures 2.1 and 2.2. Figure 2.3 shows gas mixing ratios for MLS [17].

Temperature, density, pressure, and mixing ratios of H_2O, O_3, N_2O, CO, and CH_4 are contained in this six reference atmospheres. Along with the CO_2, these are the most radiatively infrared active molecules. 21 additional species are common and they are: NO, SO_2, NO_2, NH_3, HNO_3, OH^-, HF, HCl, HBr, HI, ClO^-, OCS, H_2CO, HOCl, N_2, HCN, CH_3Cl, H_2O_2, C_2H_2, C_2H_6, and PH_3. The accompanying volume

mixing ratios compiled using direct or satellite measurements, and/or theoretical predictions [17].

The altitude increments for AFGL atmospheric constituent profiles are; 1 km between 0 and 25 km, 2.5 km between 25 and 50 km, and 5 km between 50 and 120 km [17].

2.1.4. Particle Composition of Atmosphere

Atmospheric particles are larger than atmospheric molecules (molecules have radii $<10^{-4}$ μm); however, they are still small enough to be suspended in the atmosphere for limited time [4] [8]. They vary in size, chemical composition, and shape (spheres, ellipsoids, rods, etc.); moreover, they may be composed of one or more homogeneous materials. Examples to particles are; biological particles, marine particles, meteoritic debris, crustal material, mineral dust, mineral water, smog, smoke, fine soil particles, cosmic dust, clouds, fog, mist, rain, freezing rain, hail, snow, ocean spray, sea salt etc. [21] [4].

The optical properties of aerosols are related to their size and refractive index. One can perform a number of categorizations of atmospheric particles with respect to their size and origin [4]. Here, those having diameters between 0.0002 μm and 100 μm are classified as aerosols. Aerosols are generally size-classified in two primary modes while each mode has different genesis [8]. Definitions and genesis of these modes are summarized in Figure 2.4, along with the ideal scheme of their size distributions.

Particles with diameter range 0.0002 μm < d < 2.5 μm are classified as *fine mode*. Fine mode has two sub modes; *aitken mode* (0.0002 μm < d < 0.1 μm) and *accumulation mode* (0.1μm < d < 2.5μm) [8]. The main sources of aitken particles are man-made sources such as combustion sources, or condensation or nucleation of molecules [8] [21]. Accumulation mode particles, on the other hand, are mainly formed by coagulation of smaller particles emitted from man-made combustion

sources, by condensation of easily evaporating species and by breaking up into small particles of larger soil particles [21]. They do not evolve larger particles [8]. Having diameter 2.5μm < d < 100 μm are *coarse mode* particles. They are mainly generated by mechanical processes and have natural sources; locally emitted wind-driven particulates such as; dust, soil particles, pollen, spores, sea spray over the ocean, and organic particles from vegetation. Natural sources do not always produce coarse particles. Sources such as volcanoes, biogenic processes and forest fires emit fine particles to the atmosphere as well [21].

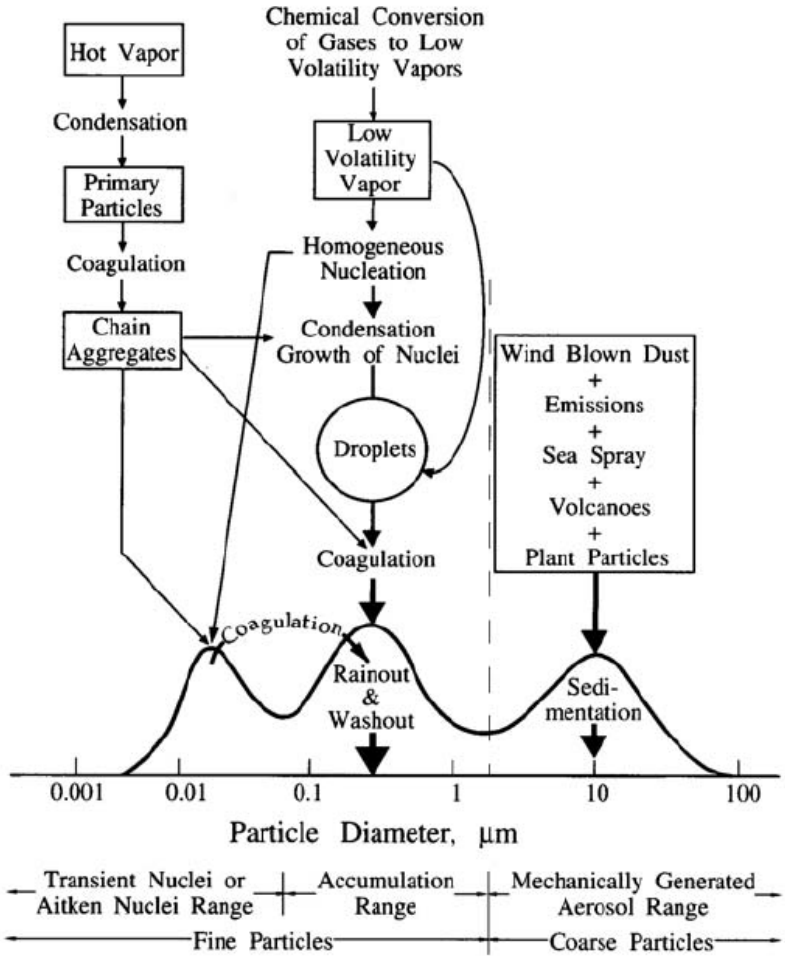

Figure 2.4. Definition, genesis and ideal size distributions of aerosols [8].

The characteristics of aerosols, consequently their optical properties, can also be substantially influenced by relative humidity. As the relative humidity increases, the water vapor condenses out of the atmosphere onto hydroscopic particles originated primarily from vegetation and sea, such as; sea salt, and aitken particles etc. This condensed water increases the size of the aerosols, and changes their composition yielding change in the refractive index. The resulting effect of the aerosols on infrared atmospheric phenomena will correspondingly be modified [9] [4].

Particles have limited residence time in the atmosphere. The residence time of aerosols is a function of their sizes. The particle removal processes include coagulation, fallout, and washout [4]. Fallout is due to effect of gravity. This effect is balanced by wind and convective currents. An aerosol's terminal velocity is the velocity at equilibrium between viscous drag due to the air, and acceleration due to gravity. Due to the vertical variability of atmospheric pressure, strong altitude dependence on terminal velocity is observed. Particles larger than ~20μm are rare, in any case [4]. Aitken mode particles are also removed from atmosphere rapidly, because they quickly coagulate (within minutes) to form coarser particles. Consequently, particles in the accumulation mode have the longest residence time in the atmosphere [21]. Aerosols are also washed out by rain or snow [4].

Size ranges, chemical nature, and sources of aerosols show considerable differences with the variations in altitude [10]. Figure 2.5 shows basic characteristics of particles as a function of altitude.

Aerosol concentrations in the troposphere generally decrease rapidly with increasing altitude [12]. In the boundary layer (0-2 km), the aerosols mainly depend on ground level and surface conditions. Thus, aerosols in this region display the highest variability with meteorological condition, climate, etc. Over the land, the aerosols are mainly wind driven soil particles, dust, and organic particles from vegetation. Aerosols over the ocean are mainly derived from sea (within a range in size from 0.3 μm to 3 μm). A smaller (residual) concentration of continental

aerosols is also present [8]. The aerosols derived from sea are mainly sea-salt particles, and are produced from sea spray and bursting bubbles, which then aggregate and condense in the high-humidity environment [8]. These producing mechanisms are highly wind dependent and require white water phenomenon [9]. Long-range global winds are capable of transporting land particles to vast distances across the oceans or continents. Those aerosols are especially associated with dust storms or large biomass fires. Thus, substantial mixing of different aerosol types may occur [10].

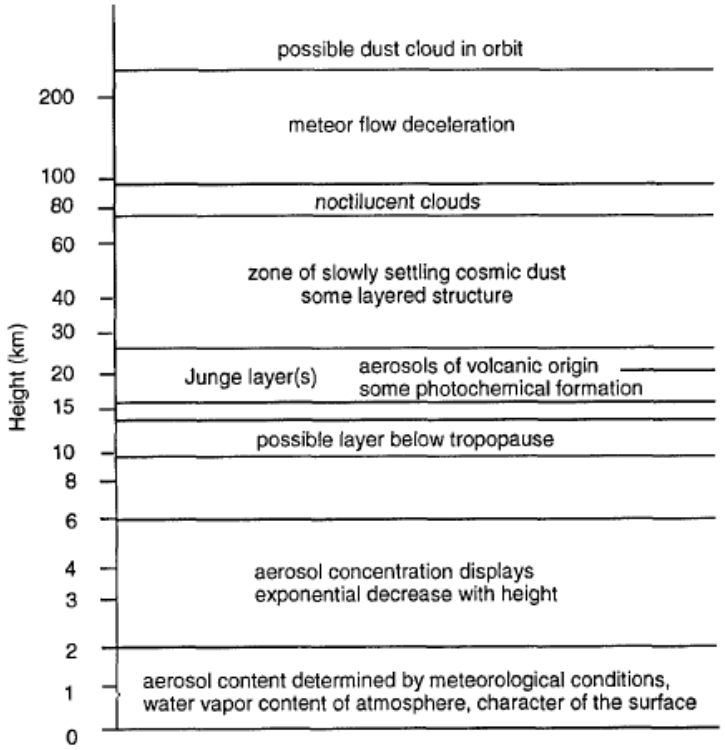

Figure 2.5. Altitude dependent characteristics of atmospheric aerosols [4].

In the troposphere, above the boundary layer, aerosol characteristics are less dependent on local surface conditions and more uniform, global distribution is observed. These aerosols are mainly coagulated gaseous species and fine dust [10].

In the region of stratosphere from 10 to 30 km, the background aerosols are mainly sulfate particles and are uniformly mixed globally. However, the aerosol concentrations can be fairly increased due to injection of dust and SO_2 by volcanic activities. Such increases in aerosol concentration may persist for several years [10].

Above the stratospheric layer, particles are mainly originated from extraterrestrial sources, such as meteoric sources [10].

2.1.5. Standard Particle Models

The description of aerosol concentration, size, and composition is technically more difficult than that of gaseous concentrations. The periodicity is also a factor in this difficulty. This renders a detailed experimental assessment in operational scenarios difficult. Thus, aerosol models are used to predict particle concentration [8]. These models describe aerosol properties as a function of meteorological or climatological parameters [9].

Altitude dependent variation of the aerosol optical properties, in general, is modeled by dividing the atmosphere into four regions. These regions have a different types of aerosol, and they are; the boundary or mixing layer (0 to 2 km), the upper troposphere (2 to 10 km), the lower stratosphere (10 to 30 km), and the upper atmosphere (30 to 100 km). Boundary layer models represent rural, urban, desert and maritime environments, rain, snow, and fog. For upper troposphere, spring-summer and fall-winter models are described. Background and volcanic conditions for spring-summer and fall-winter models are developed for lower stratosphere [9].

2.2. Radiative Transfer in the Atmosphere

A pencil of radiation traversing through the atmosphere is weakened by its interaction with the atmospheric constituents [12]. This reduction in the intensity of forward propagating radiance is named as *extinction*. Two basic processes cause extinction: *absorption* and *scattering*. Both gaseous molecules and particles absorb

and scatter radiation [4]. Besides, the intensity of propagating radiation may be strengthened by emission from the atmospheric material plus scattering from all directions into the propagation direction [12]. Thus, if the intensity of propagating radiance, L_λ, becomes $L_\lambda + d\,L_\lambda$ after traversing a distance dr, then [4]

$$dL_\lambda(r) = -\beta_{ext}\, L_\lambda(r)\, dr + J_\lambda(r) dr \tag{2.1}$$

where $L_\lambda(r)$ is the spectral radiance at a point r, $J_\lambda(r)$ is the *source term* accounting for path emission and scattering. β_{ext} is the *volumetric extinction coefficient* (cm^{-1}). It expresses the total losses by absorption and scattering per unit length along the propagation path, and is defined as [4]:

$$\beta_{ext} = \sum_i C_{ext,i}(\lambda, r)\rho_i = \sum_i \beta_{ext,i} \tag{2.2}$$

where $C_{ext,i}(\lambda)$ is the *spectral extinction cross section* of the *i*'th gas or particle (cm^2), and ρ_i is the number density of the *i*'th gas or particle (cm^{-3}). Since the extinction process is linear [7] (under the single scattering limit), the extinction coefficient can be described as the linear sum of the individual extinction processes for the *i*'th gas or particle [4]:

$$C_{ext,i}(\lambda, r) = C_{abs,i}(\lambda, r) + C_{sca,i}(\lambda, r) \tag{2.3}$$

or,

$$\beta_{ext,i} = \beta_{abs,i} + \beta_{sca,i} \tag{2.4}$$

The solution for the radiative transfer equation (Equation 2.1) is in the following form [4]:

$$L_\lambda(r) = L_\lambda(r)\exp[-\tau_{OD}(r)] + \int_0^r J_\lambda(r')\exp[\tau_{OD}(r') - \tau_{OD}(r)]dr' \tag{2.5}$$

where the τ_{OD} is the *optical depth*, and is defined as

$$\tau_{OD}(r) = \int_0^r \beta_{ext}(r')dr' \tag{2.6}$$

2.3. Definition of Atmospheric Transmittance

If the transmittance is high, the source term, $J_\lambda(r)$ (in Equation 2.5), is relatively small, and can be dropped. This leads to the simplified definition of the *atmospheric transmittance*, T_λ [4]

$$T_\lambda(r) = \frac{L_\lambda(r)}{L_\lambda(0)} = \exp[-\tau_{OD}(r)] \tag{2.7}$$

where $L_\lambda(0)$ is the source or signal radiation at point $r = 0$. Atmospheric transmittance is a unitless quantity that determines what fraction of forward propagating radiance can pass through the atmosphere within a certain range.

For a homogeneous path [4],

$$\tau_{OD}(r) = \beta_{ext} r \tag{2.8}$$

yielding the *Beer-Bouguer-Lambert law* which states that the extinction process is linear, independently in the intensity of radiation and in amount of matter, provided that the physical state (i.e., temperature, pressure, composition) is held constant [7]. It is described with the simple exponential function [12] [4]:

$$L_\lambda(r) = L_\lambda(0)\, e^{-\beta_{ext} r} \tag{2.9}$$

As a note, the atmosphere is generally assumed to be structured in plane-parallel, many homogeneous layers [4]. For example, a horizontal path at sea level can be considered as homogeneous [9].

A representative atmospheric transmittance measured over 1820 m horizontal path at sea level is shown in Figure 2.6.

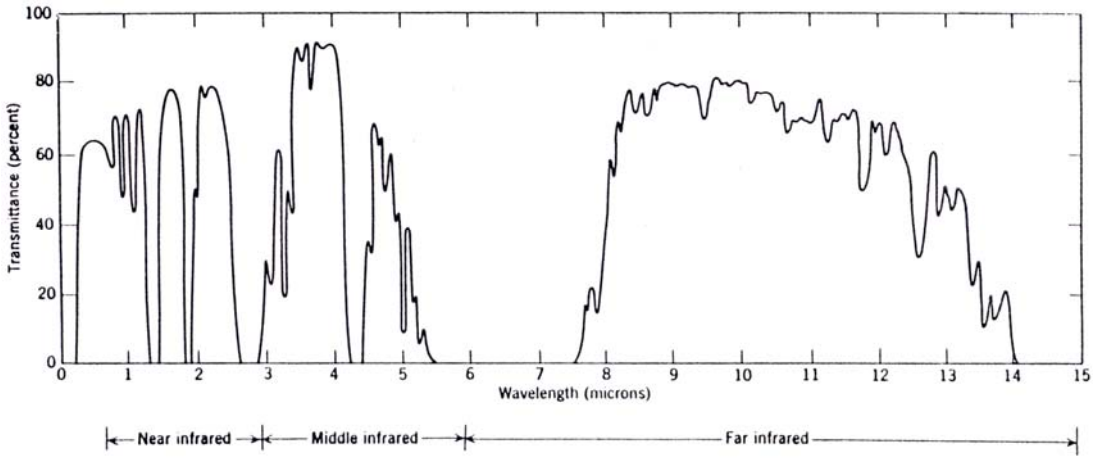

Figure 2.6. Atmospheric transmittance measured over 1820 m horizontal path at sea level [11].

The wavelength regions, where the transmittance is relatively high, are called *atmospheric windows*. Obviously, for efficient energy transfer, the wavelength of source should be well within one of these windows. There are many atmospheric windows in visible to mid-infrared region (Figure 2.6) [11]. However, variable nature of the atmosphere yields variations in transmittances of these windows; moreover, substantial variations can be observed.

Since the absorption and scattering coefficients strictly depend on the wavelength of the incident radiation, and on abundances and specific optical properties of the atmospheric constituents, one would expect that the lowest average transmittance (in the range of optical wavelengths) and the variations occur in the boundary layer of the atmosphere. Therefore, the atmospheric spectral transmittance modeling requires understanding of all photon interaction mechanisms individually.

2.4. Molecular Absorption

2.4.1. Basic Concepts

Molecular absorption is the primary factor in atmospheric propagation of optical radiation. The atmospheric window regions are defined by molecular absorption [4]. Absorption spectra of six important molecules and the simulated total absorption of the atmosphere are shown in Figure 2.7. As seen from the Figure, water vapor, carbon dioxide and ozone are the major contributors to atmospheric absorption.

The absorption of optical radiation by molecules in the atmosphere is primarily associated with individual optical absorption and thus transitions between the allowed quantized energy levels of the molecule. An interacting photon with a frequency ν_0 will cause a transition to a higher, excited state (from E_0 ground state to upper state, E_1) that can be expressed by *Planck relation* [4];

$$E_1 - E_0 = h\nu_0 \tag{2.10}$$

where h is Planck constant.

The excited state has a limited lifetime. If the absorbed photon is reemitted with a negligible conversion to translational energy, the process is one of *scattering*. However, usually, before the matter can reemit, molecular collisions occur, during which nonradiating transitions (deactivation) can take place. Then, the energy is transferred in other forms of internal energy. *Absorption* process occurs when energy is transferred to kinetic energy; moreover, the reverse process is called *thermal emission* [7]. When absorption process occurs, a spectral line is observed at frequency ν_0 because of the absence of energy relative to the incident photon field [4].

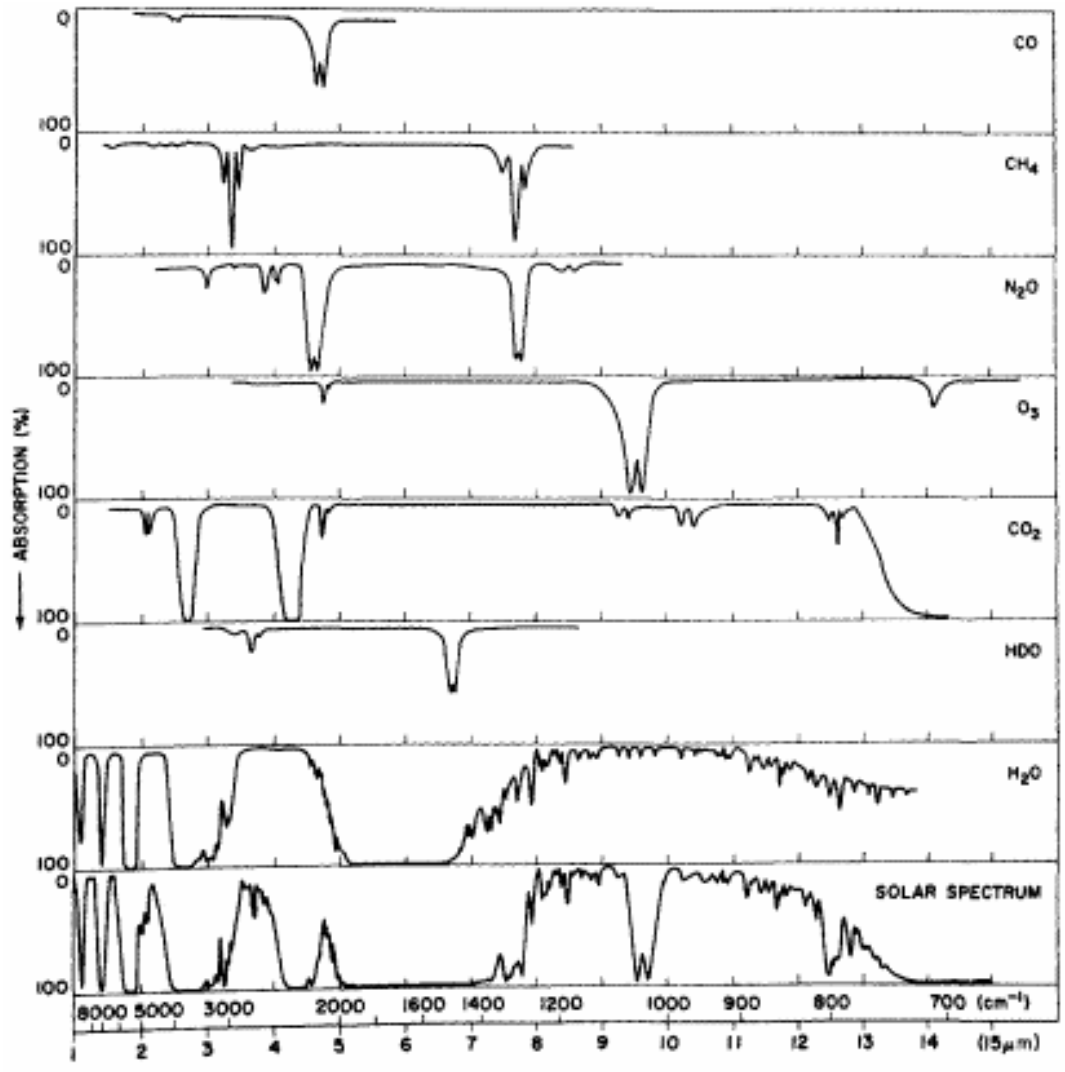

Figure 2.7. Absorption spectra of the atmosphere and six important molecules [7].

The absorption occurs not only at the resonance frequency of the transition. Over a spread of frequencies caused by broadening factors lead to a finite width of the spectral line [4]. The resulting absorption feature is shown in Figure 2.8. The frequency dependence of this absorption or the shape is often called the *lineshape* (Figure 2.8). The lineshape of a single transition is commonly characterized by several parameters including the *line-center* (ν_0), *line strength* or line intensity (S), and *line-width* or half-width (α). For a molecule, the absorption coefficient of

the *i*'th line can be broken down into two factors, the *line-strength*, and the *line-shape function*, $g(\nu,\nu_0;\alpha_i)$ [4]:

$$\beta_{abs,i}(\nu) = S_i\, g(\nu,\nu_0;\alpha_i) \tag{2.11}$$

where ν denotes wave number (or frequency).

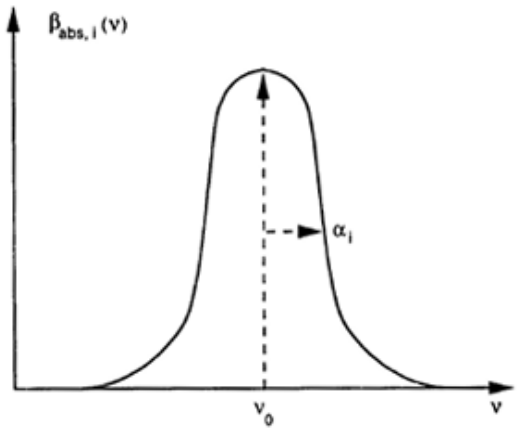

Figure 2.8. Lineshape of molecular absorption [4].

The molecules include several absorption lines. Therefore the total absorption coefficient for a molecule is [4]

$$\beta_{abs} = \sum_i \beta_{abs,i}(\nu) = \sum_i S_i g(\nu,\nu_i) \tag{2.12}$$

Linewidth is defined as; half of the frequency interval between ν_0 and the frequency at which $\beta_{abs,i}(\nu)$ has fallen to one half of its maximum value. Linewidth values in the Earth's atmosphere can range from 0.0002 cm^{-1} (for isolated molecules) to 0.5 cm^{-1} (in the high atmospheric pressures). The important broadening effects, each having its own lineshape function, in terrestrial atmosphere are listed in follows [12] [7].

- Damping of oscillator vibrations resulting from the loss of energy in emission. In this case, the broadening of lines is considered to be normal. This is called *natural broadening* and described by Lorentzian lineshape. The linewidth is inversely proportional to the lifetime of a molecule at any given energy level. Due to relatively long lifetimes of undisturbed molecules, resulting linewidth is very small, with values in the order of 10^{-5} cm^{-1}.

- Perturbations due to collisions between absorbing molecules and between the nonabsorbing and absorbing molecules. This is known as *pressure broadening* and is described by Lorentzian lineshape. For an atmospheric gas at room temperature and pressure, a typical linewidth value is about 0.05 cm^{-1}.

- Shifts in observed frequencies due to the differences in thermal velocities of atoms and molecules. This is called *Doppler broadening.* Unlike in natural and pressure broadening processes, it is an inhomogeneous process described by Gaussian lineshape. If the temperature is high enough to produce molecular motion, and the pressure is low enough so that molecular collisions, which terminate dipole moment oscillation, do not occur. At pressures about 0.007 atm or less, Doppler broadening predominates with a typical linewidth of 0.001 cm^{-1} at 296 K.

The broadening of lines due to natural broadening is negligible as compared to that caused by pressure and Doppler broadenings. In the upper atmosphere, pressure and Doppler broadenings are considered; however, in the lower atmosphere (below about 20 km), pressure broadening prevails [12].

The line strength is a direct measure of the ability of a molecule to absorb photons corresponding to a given transition. It is defined by the entire area (S_i) under the absorption curve [4]:

$$S_i = \int_0^\infty \beta_{abs,i}(\nu) d\nu \tag{2.13}$$

While the lineshape is generally determined by the molecules' environment, the resonant frequency and the strength of the absorption are determined mainly by the structure of the molecule; nature of the intramolecular bond and by the configuration and mass of the atoms forming the molecule [4] [7]. In radiative transitions, the molecules must couple with an electromagnetic field, so that energy exchanges can take place. This coupling is often provided by the electric dipole moment of the molecule. Dipole moment can exist if the effective centers of the positive and negative charges of the molecule have nonzero separation [12].

The strength of the transition is partially determined by the strength of the electric dipole moment. For rotational and vibration-rotation spectra, line positions of the transitions are determined by the masses of the atoms, the relative positions, and the bond strengths [4].

A molecule can store various energies. Moving particles in space have kinetic energy due to their motion in space. This is *translational energy*. Molecules can rotate, or revolve, about an axis through its center of gravity. Thus they have *rotational energy*. Atoms of a molecule are bounded by certain forces like springs; the individual atoms can vibrate about the equilibrium positions relative to one another. This indicates that a molecule has *vibrational energy*. The energy of a molecule changes as a result of a change in the energy state of the electrons of the atoms. Therefore, the molecule has *electronic energy*. The last three types of energy are quantized and can only take discrete values governed by selection rules. The absorption and emission processes can take place when the atoms or molecules undergo transitions from one energy state to another [12].

Rotational energy changes are relatively small. Thus, pure rotational lines occur in the microwave and far-infrared regions (1-100 cm^{-1} or 10^2-10^4 μm) [12] [7].

Vibrational energy changes are often much greater than the minimum changes in rotational energy [12]. Vibrational lines are in the near- to far-infrared bands (10^4-10^2 cm^{-1} or 1-100 μm) [7].

Electronic transitions typically have a few electron volts of energy. Since a high-energy photon is required for this transition, emission and absorption often occur in the ultraviolet (strong absorption bands, which determine the end of atmospheric transmittance), visible (weak bands), and near-infrared regions of the spectrum (10^5-10^4 cm^{-1} or 0.1-1 μm) [12] [7].

Rotational spectra in infrared region require molecules with permanent dipole moments (e.g., H_2O, O_3, CO, and N_2O). Such molecules are called *polar* molecules. Spherical symmetric molecules are called *nonpolar* molecules, have no electric dipole moment (e.g., N_2, O_2, CO_2, and CH_4), and have no rotational spectra [4].

Vibrational spectra in infrared region require molecules with only a change in dipole moment that is caused by asymmetric relative positions of the atoms within the molecule. For this reason, if the relative vibrational motion of the atoms within a nonpolar molecule is asymmetrical, then a dipole moment may be produced and vibrational spectra can exist. Polar molecules are typically strong absorbers of infrared radiation and they have spectra from the far-infrared (pure rotational) throughout the mid-infrared (vibrational-rotational bands) [4]. Examples of vibrational motions of some important atmospheric molecules are illustrated in Figure 2.9.

Molecular vibrations produce oscillating electric dipole moment, which is enough for both vibrational and rotational transitions. Therefore, the vibrational energy changes do not occur alone; both vibrational and rotational transitions occur simultaneously. The resulting energy level is the sum of the separate transition energies. The spectrum of the combined transitions is an array of rotational lines grouped around the vibrational frequency. This constitutes a group of lines called

vibrational-rotational band in the intermediate infrared spectrum [12]. Similarly, vibrational and rotational changes will accompany an electronic change [7].

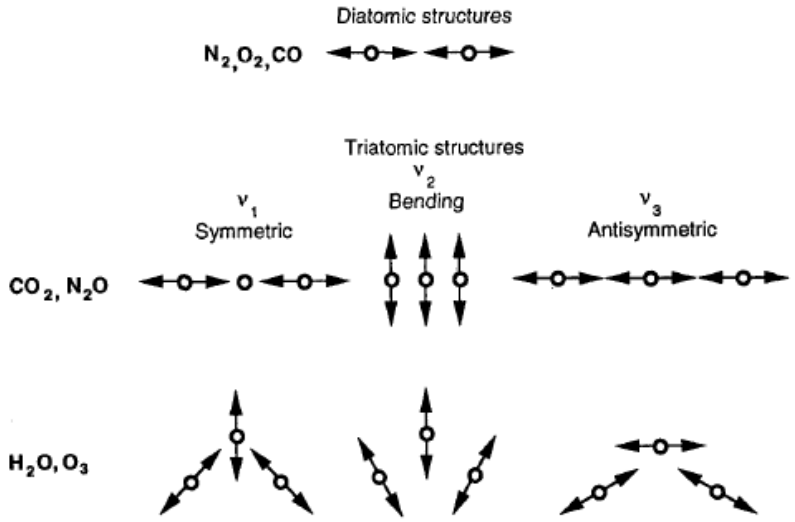

Figure 2.9. Configurations and vibrational modes of diatomic and triatomic atmospheric molecules [4].

Vibrational-rotational optical absorption lines (or bands) are some of the most distinctive and identifiable absorption lines of many atmospheric molecules in the infrared spectral region [10]. For example, the importance of water vapor molecule is due to these bands [4].

It should be noted that, at infrared frequencies, only molecules can strongly couple to the electromagnetic field. Atoms do not have rotational and vibrational spectra [4].

The locations of the vibrational frequencies determine the atmospheric windows [4]. The centers of the most important absorption bands are listed in Table 2.3.

Table 2.3. The centers of the most important vibrational absorption bands [22].

Molecule	Vibrational mode	Band center in cm^{-1}
H_2O	Bend	1595
H_2O	Symmetric O-H stretch	3657
H_2O	Antisymmetric O-H stretch	3756
CO_2	Bend	667
CO_2	Antisymmetric C-O stretch	2349
O_3	Bend	701
O_3	Antisymmetric O-O stretch	1042
O_3	Symmetric O-O stretch	1103
N_2O	Bend	589
N_2O	N-O stretch	1285
N_2O	N-N stretch	2224
CO	C-O stretch	2143
CH_4	Degenerate deformation	1306
CH_4	Degenerate stretch	3019

2.4.2. Molecular Spectroscopic Database

HITRAN [23] (HIgh-Resolution TRANsmission Molecular Absorption Database) is one of the spectral line databases available which provide a compilation of the line centers, strengths, and widths as well as several other important parameters such as the lower state energy, pressure induced line center shifts, isotopic abundances, rotational and vibrational quantum indexing, width-temperature exponents, and transition probabilities. It is a long-running project started by the Air Force Cambridge Research Laboratories (AFCRL) in the late 1960's [24]. The HITRAN compilation consists of several components that serve as input for radiative transfer calculation codes: individual line parameters for the microwave through visible spectra of molecules in the gas phase; individual line parameters and absorption cross-sections for bands in the ultra-violet; refractive indices of aerosols. The parameters included in HITRAN are sometimes direct observations, but often calculated results of various quantum-mechanical solutions. The current edition of

HITRAN contains spectroscopic parameters for 39 molecules including many of their isotopes [23].

2.5. Atmospheric Scattering

2.5.1. General Aspects

Scattering is simply the interaction of photons with particles or molecules causing a redirection of observed photon energy [7]. Both molecules and particles are responsible for scattering. Scattering causes two basic considerations in optical atmospheric phenomena; the radiation can be scattered through the line-of-sight contributing radiance, and scattering causes a reduction in the intensity of forward propagating beam [4] [25]. Extinction by molecular scattering (Rayleigh scattering) is mainly effective on atmospheric transmittance from visible to near infrared (especially <1μm) region [26]. However, extinction by particle scattering is effective from visible throughout the infrared region; moreover, it can drastically reduce the incident radiance intensity. Representative aerosol extinction (both absorption and scattering included) and molecular scattering coefficients are shown in Figure 2.10.

Scattering phenomenon is treated mostly by classical electromagnetic theory. Even though, the matter may be continuous and is electrically neutral in many cases, it is composed of discrete electric charges. Electromagnetic field can excite the charges in matter to oscillate. Oscillating charges radiate electromagnetic waves, which are scattered waves; briefly, an incident wave from the source excites secondary waves from the scatterer. The superposition of all scattered waves (by interaction of all incident waves) is what is observed. If the frequency of scattered waves is that of the source, scattering is said to be *elastic* (or coherent) [27].

Scattering of light may be classified in terms of two theoretical frameworks; Rayleigh and Mie scattering theories. Rayleigh scattering is applicable to small, dielectric (non-absorbing) spherical particles, namely molecules. Mie scattering

covers the general spherical scattering solution (non-absorbing or absorbing) without a precise boundary on size of particle. Therefore, Mie scattering does not have size limitations and converges to the limits of geometrical optics for large particles [28]. In fact, Mie scattering includes Rayleigh scattering. Rayleigh scattering is an approximation of Mie theory where the particle radius shrinks to zero [27]. However, Rayleigh scattering theory is generally preferred for molecules due to the complexity of the Mie scattering formulation.

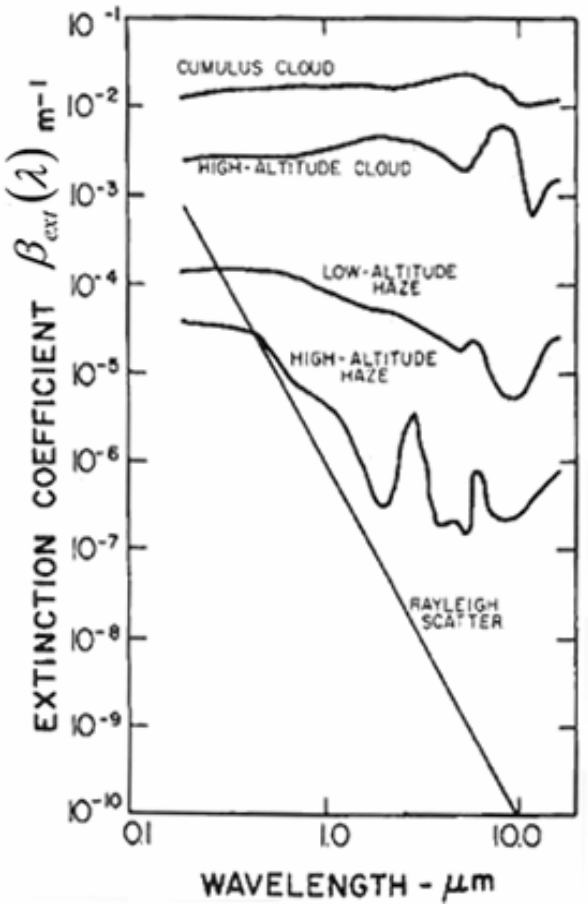

Figure 2.10. Measured aerosol extinction and molecular scattering coefficients as a function of wavelength (Adopted from [10]).

Scattering phenomenon is strictly dependent on the size of the scatterer and on the wavelength of the incident electromagnetic radiation. For aerosol scattering, composition is another important factor. A representation of scattering for differing scatterer sizes is shown in Figure 2.11.

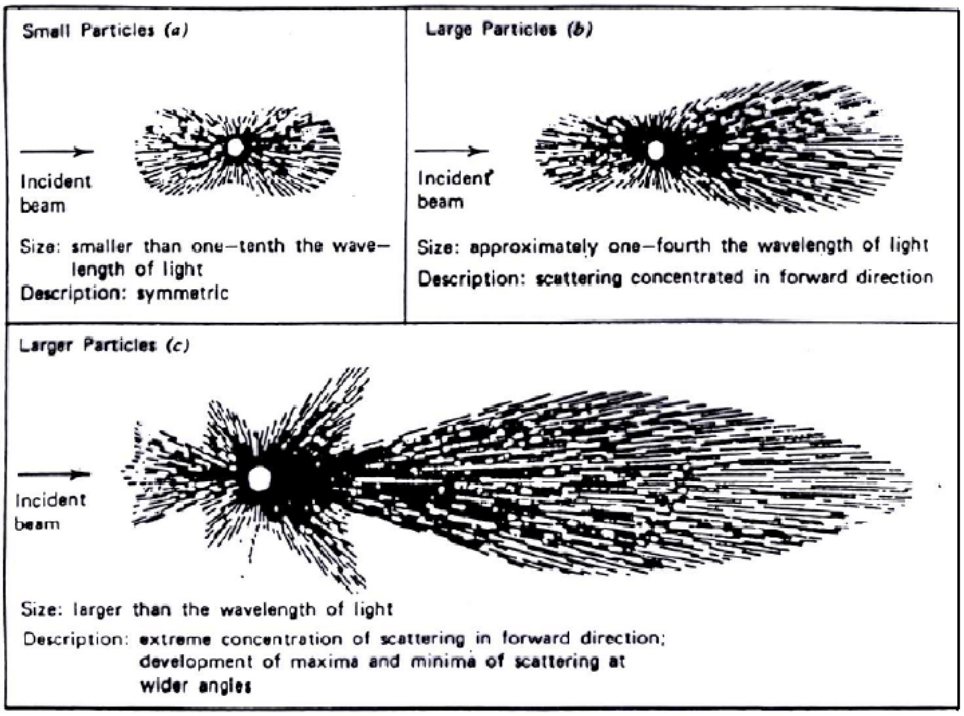

Figure 2.11. Scattering by differing sizes of particles [29].

2.5.2. Molecular Scattering (Rayleigh Scattering)

Molecular scattering is an elastic scattering of the light that is responsible for the blue color of the sky. It originates from the dipole moment which is synchronously perturbed by the incident radiation [4]. Considering the radiation at the position of the particle as an oscillating homogeneous electric field, the charges of the particle tend to reallocate themselves in the direction of the field. Thus an electric dipole is

formed which is oscillating with the same frequency as the incoming light. Rayleigh assumed that scattering by air molecules can be described as the irradiation of this dipole [7].

The Rayleigh scattering cross section (simply the scatter coefficient) per unit volume is given by [4];

$$\beta_{sca}(z) = \frac{8\pi^3 \left(n^2 - 1\right)^2 N(z)}{3N^2(0)\lambda^4} \frac{(6+3\delta)}{(6-7\delta)} \tag{2.14}$$

where δ is the depolarization factor arising from the anisotropy of the gas molecule (most of the atmospheric molecules have linear structure). For air, a commonly accepted δ value is 0.035 [4]. The value of 0.0279 is also given for dry air (i.e. no moisture included) [9]. $N(z)$ is the number density of the gas molecules at height z, λ is the wavelength of the optical radiation, and n is the refractive index of the medium [4]. As seen from the equation, shorter wavelength light is more strongly scattered out than longer wavelength light [10].

2.5.3. Mie Theory (Absorption and Scattering by Particles)

Mie theory treats scattering of light by homogeneous spherical dielectric particles of arbitrary dimensions. Each particle is treated as being isolated from all its neighbors. The intensity of the scattered light can be calculated depending on its wavelength, the scattering angle, the radius and the complex refractive index of the particle [4].

The critical input parameters in Mie Theory are particle size and wavelength. A key parameter which illustrates the nature of the Mie calculation is the dimensionless size parameter, x [4];

$$x = \frac{2\pi r}{\lambda} \tag{2.15}$$

where r is the radius of the particle, and λ is the wavelength of the incident light. As a note, for particles with $r \ll \lambda$, the Mie Theory approximates to the Rayleigh scattering [27].

The extinction cross section for a single particle is the sum of the absorption and scatter cross sections [4];

$$C_{ext} = C_{sca} + C_{abs} \tag{2.16}$$

where the sub indices *ext*, *sca*, and *abs* represent extinction, scattering, and absorption, respectively. *Scattering efficiency* and *extinction efficiency* are defined as the normalizations of cross sections to the geometric cross section for a sphere (πr^2) [4],

$$Q_{sca} = \frac{C_{sca}}{\pi r^2} \tag{2.17}$$

$$Q_{ext} = \frac{C_{ext}}{\pi r^2} \tag{2.18}$$

The Mie solutions for scattering and extinction efficiencies are given as [7],

$$Q_{sca} = \frac{2}{x^2}\sum_{n=1}^{\infty}(2n+1)\left(|a_n|^2 + |b_n|^2\right) \tag{2.19}$$

$$Q_{ext} = \frac{2}{x^2}\sum_{n=1}^{\infty}(2n+1)\mathrm{Re}\left(a_n + b_n\right) \tag{2.20}$$

where a_n and b_n are complex Mie coefficients. These coefficients are functions of complex refractive index of the particle, m ($m = n + in'$), and of Ricatti-Bessel functions of the size parameter, x (given in 2.15).

Calculated absorption, scattering, and extinction efficiencies [30] are shown in Figure 2.12 for a wet sea salt particle (refractive index, n=1.29+*i*0.05) having radius of 1 μm. As seen from the Figure 2.12, scattering efficiency is maximum at wavelength that is about the radius of the particle, and decreases as the wavelength increases.

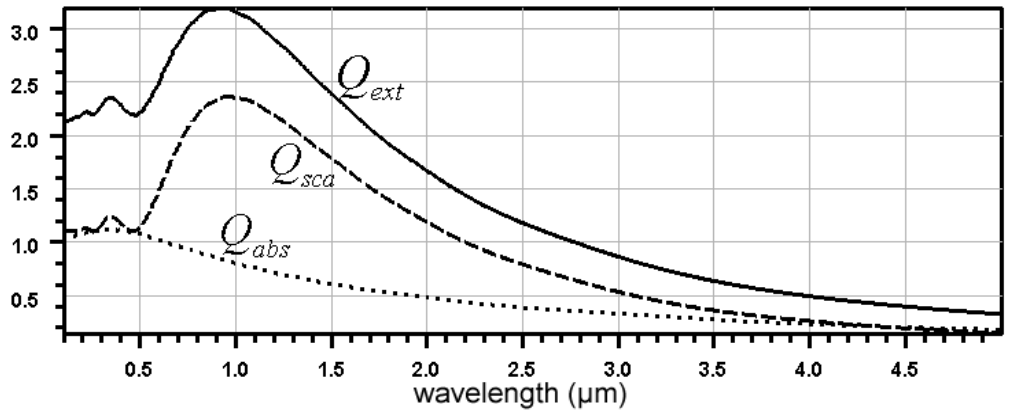

Figure 2.12. Mie efficiencies for a wet sea salt particle (particle radius is 1 μm, and refractive index is 1.29+*i*0.05).

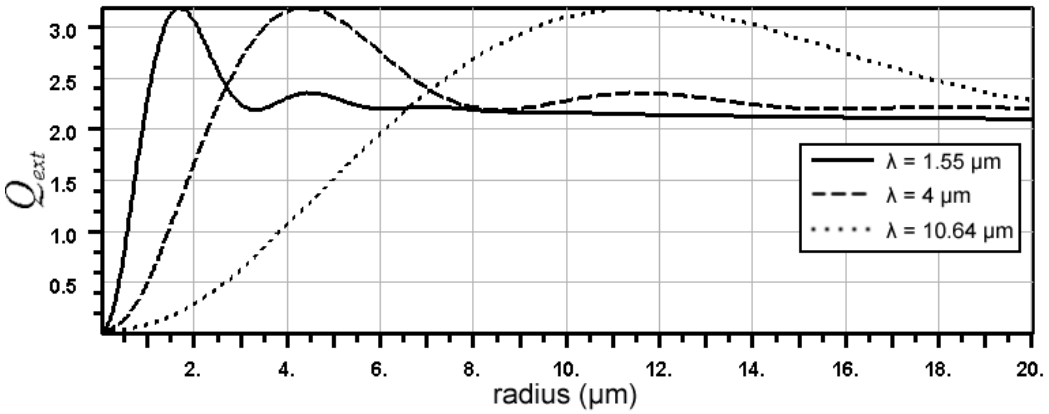

Figure 2.13. Mie extinction efficiencies as a function of particle radius for different wavelengths for a wet sea salt particle (refractive index is 1.29+*i*0.05).

Figure 2.13 shows calculated extinction efficiencies [30] as a function of radius for differing wavelengths for a wet sea salt particle (refractive index, n=1.29+*i*0.05) [30]. As seen from the Figure 2.13, extinction efficiencies are maximum at wavelength that is about the radius of the particle, and has an average decrease as the wavelength increases.

Since the atmospheric particles only exist as a mixture having various radii, the macroscopic scattering (β_{sca}) and extinction (β_{ext}) coefficients are the integration over the particle size distribution function, n(r) [7];

$$\beta_{sca} = \int_0^\infty Q_{sca}(r)\pi r^2 n(r)dr \tag{2.21}$$

$$\beta_{ext} = \int_0^\infty Q_{ext}(r)\pi r^2 n(r)dr \tag{2.22}$$

The size distribution function $n(r)$ is defined as the number of particles per unit volume with radii between r and $r + dr$.

2.5.4. Navy Maritime Aerosol Model

In this study, for optical properties of over ocean aerosols, Navy Maritime (NAM) aerosol model is used. This model is one of the standard empirical aerosol models. It describes the size distribution of aerosol particles close to the surface (of 10 meters altitude) of open ocean. It depends on four parameters; dimensionless *air mass parameter* (relative units), *average wind speed* (m/s) during the last 24 hours, *current wind speed* (m/s), and *relative humidity* (%) [31]. The size distribution function, $n(r)$, is completely specified by these four parameters. The extinction, absorption, scattering coefficients are determined by using Mie Theory.

The model differentiates between three types of aerosols suggesting that marine atmosphere is a composition of three distinct populations, each having different size distributions and refractive indices [9].

The smallest of aerosols is the continental component that describes background aerosol. It has little to do with current wind speed; however, it depends on the elapsed time required for the air mass to traverse the sea from the continent to the point of observation [9]. Because of the difficulties in qualification of this component by meteorological parameters, an integer from 1 to 10 is used to specify the air mass parameter input. It states the qualitative indication of the continental component. A value 1 represents the relatively pure maritime aerosol, and a value of 10 represents a significant continental component [9].

The second component represents the stationary component of the maritime aerosol. It is the part of the maritime aerosol that is dependent on the current and the history of the wind speed. It stands for the high wind and white water phenomenon but do not fall out rapidly. This component is related to the average wind speed over the past 24 hours [9].

The third component is the fresh component of the model. It is related to the current wind speed, and reflects the current action of the production of drops produced by white water, because of wind and wave actions [9].

The characteristic of sea salt particle is highly dependent on relative humidity. In the model, radii of the three components are modified by relative humidity, while the total number of particles is not altered [9].

There are some limitations in the model; relative humidity between 50% and 98%, and wind speed (both for current and past 24 hour averaged) between 0 and 20 m/s [9].

CHAPTER 3

CALCULATIONS AND DISCUSSIONS

In this chapter, determination of the desired wavelength interval(s) at which the atmospheric transmittance (AT) is relatively high, and have relatively low dependence on variations in temperature, relative humidity, wind speed and atmospheric pressure, under the conditions given in Table 3.1. For the study, the range of wavelengths, 0.3-14 μm have been scanned throughout the work.

Table 3.1. Assumed conditions for the calculations.

Atmospheric condition	Clean (includes no fog, rain, or snow etc.)
Earth surface	Sea surface
Path geometry	Horizontally aligned to earth surface
Path altitude	10 meters
Path length	15 km

At first, a geographical region is determined, and the required information about the atmospheric constituents is collected. Then, the variations in AT due to the periodically measured meteorological parameters are calculated. Finally, individually calculated affects of these meteorological parameters on AT are gathered in order to determine the desired wavelength interval(s).

3.1. Selection of Location and the Compilation of Atmospheric Parameters

Under the assumption that the atmosphere can be considered as sliced into many homogeneous layers [9], neglecting the earth curvature effects, the horizontal path at nearly sea surface is considered as homogeneous in this study. Since the atmosphere over sea surface is considered, the geographical location is selected to be Alanya region which is located at the south coastal zone (Eastern Mediterranean) of Turkey.

Pressure, temperature, relative humidity, and wind speed are measured periodically at Alanya meteorological station [6]. However, gas concentrations are not measured periodically at the location. Therefore, basic contributor gas concentrations (CO_2, CH_4, CO, O_3, and N_2O) are taken from other mid latitude stations [32]. For the rest of the gas concentrations, AFGL mid latitude atmospheric constituent profiles [17] are used (see section 2.1.3). For aerosol size distributions over sea surface; the relative humidity, wind speed, and continental aerosol dependent “Navy Maritime” (NAM) aerosol model [31] is used (see section 2.5.4). Summary of the suitable data is given in Tables 3.2, 3.3, and 3.4.

As seen from the Table 3.3, for summer and winter seasons, the range of the values of pressure and relative humidity are approximately similar. However, the highest difference is seen in temperature and wind speed.

Table 3.2. Atmospheric parameters [6] [32] [17] [31].

Requirement	Source
Meteorological parameters : temperature, pressure, relative humidity, wind speed.	Alanya Meteorological Station, Location : At the south coastal zone (Eastern Mediterranean) of Turkey Latitude : 36.55N Longitude : 32E Elevation : 10m Frequency of measured data : once per 3 hours
CO_2	Station: Sede Boker, Israel Latitude: 31 7' N Longitude: 34 52' E Altitude: 400 m
CH_4	
CO	
O_3	Station: Giordan Lighthouse, Malta Latitude: 36 4' N Longitude: 14 13' E Altitude: 167 m
N_2O	Station: Lampedusa, Italy Latitude: 35 31' N Longitude: 12 38' E Altitude: 45 m
Gas mixing ratios other than listed above	Mid Latitude Summer (MLS) and Mid Latitude Winter (MLW) atmospheric constituent profiles.
Aerosol size distributions	Navy Maritime (NAM) standard aerosol model

Table 3.3. Meteorological parameters for Alanya [6].

Winter Season (1 December 2004 – 28 February 2005)				
	Minimum	*Maximum*	*Arithmetic Mean*	*Standard Deviation*
Pressure (mbar)	999.9	1029.7	1017.02	5.89
Temperature (C^0)	5	21.67	13.29	3.24
Relative Humidity (%)	19.98	100	59.16	15.93
Wind Speed (m/s)	0 (calm atmosphere)	11.62	1.77	1.09
Summer Season (1 June 2005 – 31 August 2005)				
	Minimum	*Maximum*	*Arithmetic Mean*	*Standard Deviation*
Pressure (mbar)	1002.2	1016.6	1007.78	2.65
Temperature (C^0)	20	35	27.99	2.90
Relative Humidity (%)	18.88	93.68	68.64	10.8
Wind Speed (m/s)	0.45	4.47	1.63	0.87

Table 3.4. Used mixing ratios of CO_2, CH_4, CO, O_3 and N_2O [32].

	CO_2 (ppmv)	*CH_4 (ppmv)*	*CO (ppmv)*	*O_3 (ppmv)*	*N_2O (ppmv)*
Winter	382.87 (Mean value Dec. 2004)	1.85825 (Mean value Dec. 2004)	0.15651 (Mean value Dec. 2004)	0.0445 (Mean value Dec. 2004)	0.318 (Mean value Dec. 2002)
Summer	378.33 (Mean value June 2004)	1.84750 (Mean value June 2004)	0.12928 (Mean value June 2004)	0.0603 (Mean value June 2004)	0.319 (Mean value June 2002)

3.2. Preparation for Calculations

The effect of each meteorological parameter (pressure, temperature, relative humidity, and wind speed) on AT is to be determined individually. Thus, while other meteorological parameters are held at seasonally arithmetic mean values, two calculations are done with the minimum and maximum values of the specified meteorological parameter. This approach will help us to determine how an individual meteorological parameter affects the AT. Besides, arithmetic mean values of all meteorological parameters are considered to determine the seasonal average transmittance. The planned calculation is shown in Table 3.5.

Table 3.5. Algorithm for the atmospheric transmittance calculations.

The meteorological parameter whose effect on AT is to be determined	*Temperature*	*Pressure*	*Relative Humidity*	*Wind speed*
Temperature	Min Max	Mean	Mean	Mean
Pressure	Mean	Min Max	Mean	Mean
Relative humidity	Mean	Mean	Min Max	Mean
Wind speed	Mean	Mean	Mean	Min Max

The calculation summary listed in Table 3.5 indicates totally eight individual atmospheric transmittance calculations. This summary is for one case only. All these nine calculations are repeated for each season (winter and summer).

Because of the restrictions of NAM aerosol model (see Section 2.5.4) [9], relative humidity values that exceed the limits (above 50% and below 98%) will be revised to limit values.

As mentioned in Section 2.5.4, the aerosol characteristics; and as a consequence, the AT depends on the distance between the continent and the observer over the ocean. The dependence of AT on continent-observer distance is proposed by the input parameter of NAM aerosol model; *continental component*, or a*ir mass parameter* which is the determinative of the qualitative degree of continental aerosol influence [9]. In order to cover the continental influence in this study, all the calculations must be done by taking the air mass parameter to be 1 (relatively pure maritime aerosol), 5, and 10 (significant continental component).

It is assumed that the seasonal minimum and maximum values of the measured meteorological parameters will cover the range those for the open sea.

3.3. Atmospheric Transmittance Calculations

The usage of all atmospheric information mentioned in Section 3.2 can be summarized as follows. Pressure, temperature, and gas mixing ratios (includes H_2O partial pressure obtained from relative humidity values) are used for molecular absorption and molecular scattering calculations. Relative humidity, and wind speed are injected into NAM standard aerosol model for the calculations of aerosol scattering and absorption. The other requirements of NAM are average wind speed for the past 24 hours, and air mass parameter. For the average wind speed, under the assumption that the current wind speed can represent the average past 24 hour wind speed, the same values of wind speed are used as well.

The AT's represented in following figures are calculated by using MODTRAN (Moderate Resolution Transmittance Code) [9] software (see Appendix B) with the defined algorithm given in Table 3.5. In this section, the AT's are presented only for air mass parameter of 5.

The effect of temperature variations on AT are shown in Figure 3.1, and Figure 3.2 for winter and summer seasons, respectively. As seen in Figures 3.1 and 3.2, effect of temperature on transmittance differs seasonally due to temperature differences between two seasons. With increasing temperature, transmittance is reduced. Dependence of AT on temperature is much greater for the wavelengths longer than 4.5 μm. This is because of the water vapor absorption (See Figure 2.7). The band centered at 1595 cm^{-1} (6.25 μm) is the most important vibrational-rotational band of water vapor (See Table 2.3). The resulting absorption caused by this band is continuous (especially in the wavelength region from 8.33 μm to 12.5 μm) resulted from the accumulated absorption of the distant wings of water vapor lines. This absorption is caused by the collision broadening (pressure broadening) between absorbing molecules (H_2O-H_2O) and between absorbing and non-absorbing molecules (H_2O-N_2). It is also suggested that contributions to continuous absorption is caused by water dimer [($H_2O \cdot H_2O$)]. Absorption of water dimer is significantly dependent on temperature and water vapor pressure [12].

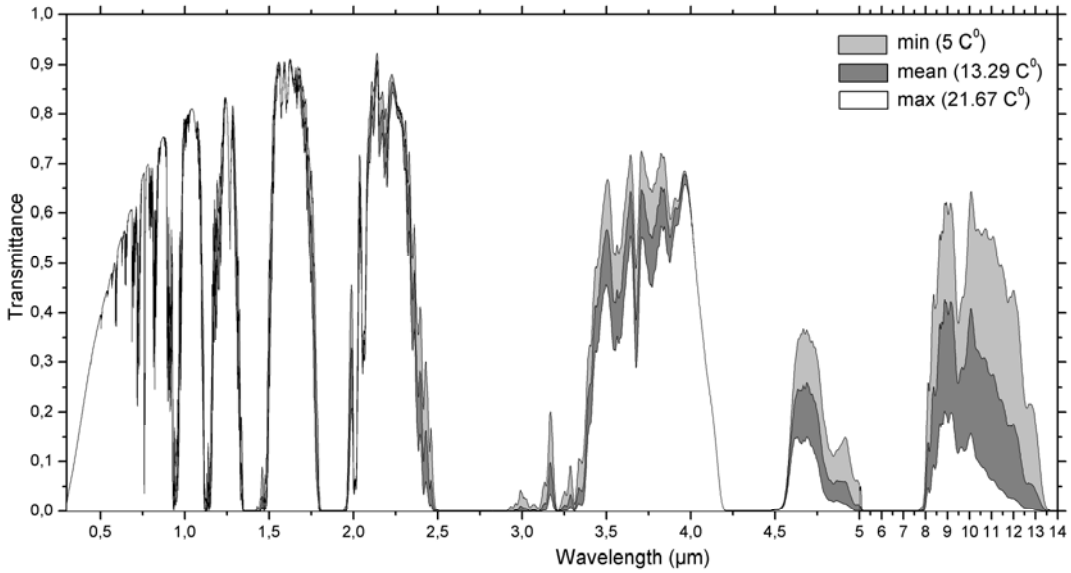

Figure 3.1. The effect of temperature on atmospheric transmittance in winter season (December 2004 – February 2005).

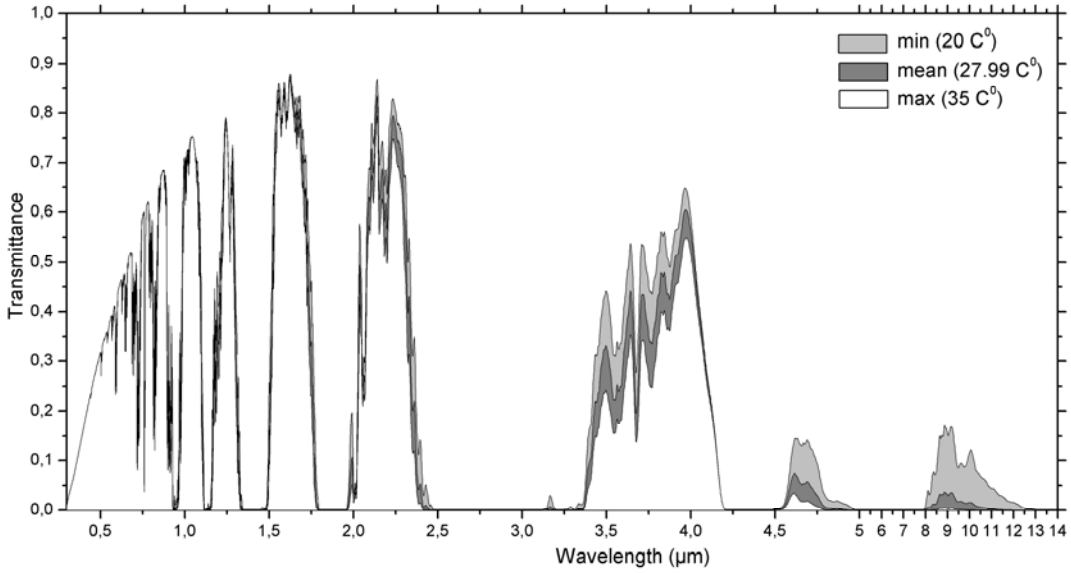

Figure 3.2. The effect of temperature on atmospheric transmittance in summer season (June 2005 – August 2005).

In Figures 3.3 and 3.4, the dependence of AT on relative humidity are shown. As seen in Figure 3.3 and Figure 3.4, AT is inversely proportional to relative humidity as it is in the temperature effect. Especially AT below 2.5 μm is more influenced by seasonal relative humidity variations. The decrease in AT due to relative humidity increase is mainly because of aerosol scattering. As mentioned in Sections 2.5.3 and 2.5.4, increase in relative humidity changes optical properties of aerosols due to condensation of water vapor out of the atmosphere onto aerosols. Additionally, Mie theory indicates that aerosols with sizes about equal to wavelength are more effective in scattering than are smaller or larger ones. Since the marine aerosol population with smaller sizes (especially 0.3-3 μm [4]) is more abundant [33], the aerosol scattering and similarly the relative humidity are more effective on AT at smaller wavelengths. The AT, at wavelengths longer than 4.5 μm, is also strongly affected by increase in relative humidity due to the continuous water vapor absorption as mentioned previously.

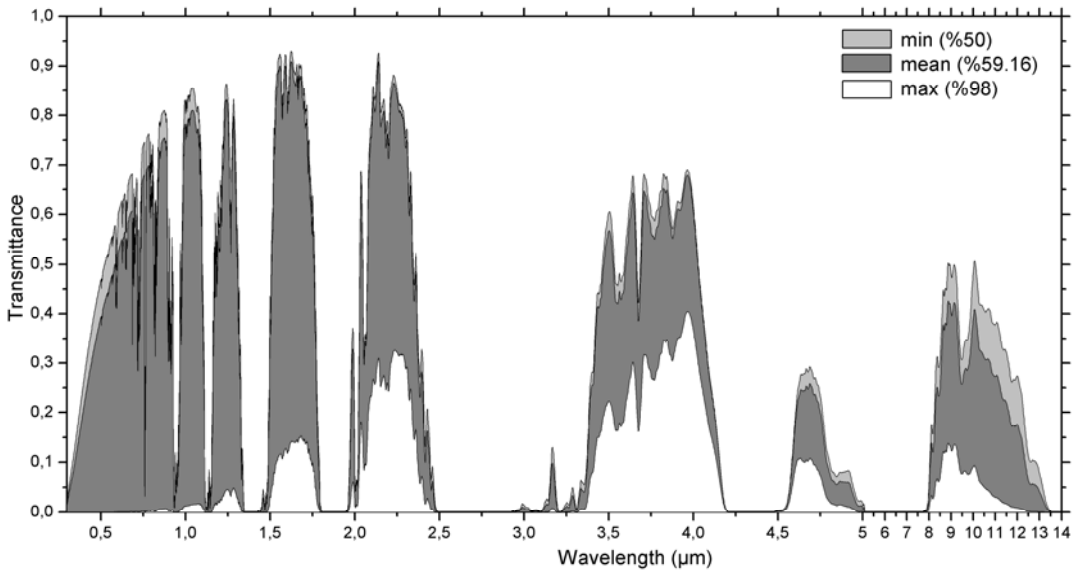

Figure 3.3. The effect of relative humidity on atmospheric transmittance in winter season (December 2004 – February 2005).

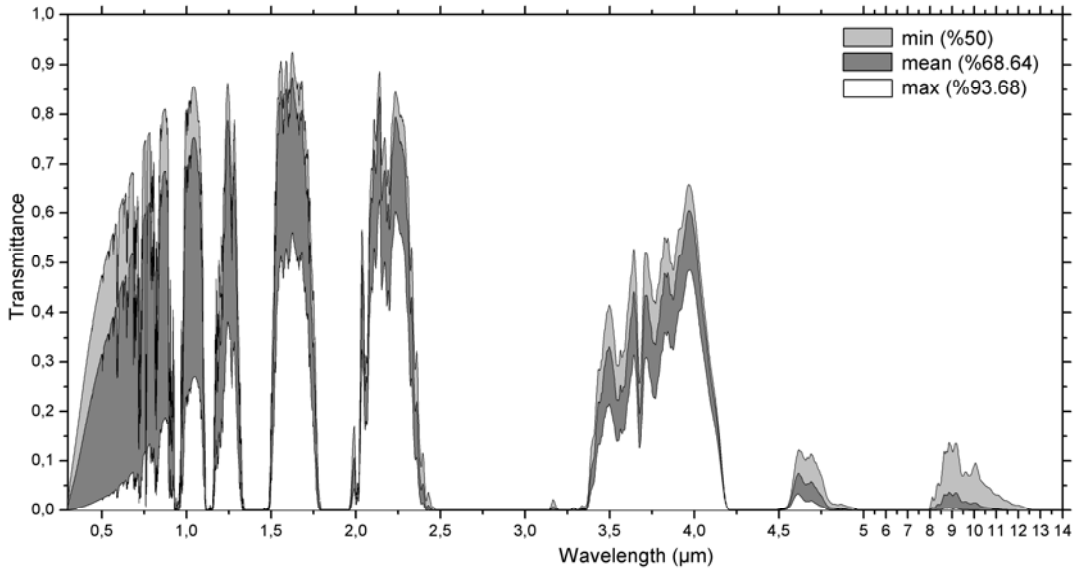

Figure 3.4. The effect of relative humidity on atmospheric transmittance in summer season (June 2005 – August 2005).

Figures 3.5 and 3.6 show the dependence of AT on wind speed. As seen in Figures 3.5 and 3.6, as the wind speed increases, AT decreases. The effect of wind speed on AT is more clearly seen in winter season due to higher seasonal maximum wind speed value. The reason of the decrease in AT due to increase in wind speed is because of aerosol extinction. As mentioned in Sections 2.1.4, and 2.5.4, aerosol concentration is proportional to wind speed. As the wind speed increases, aerosol extinction increases.

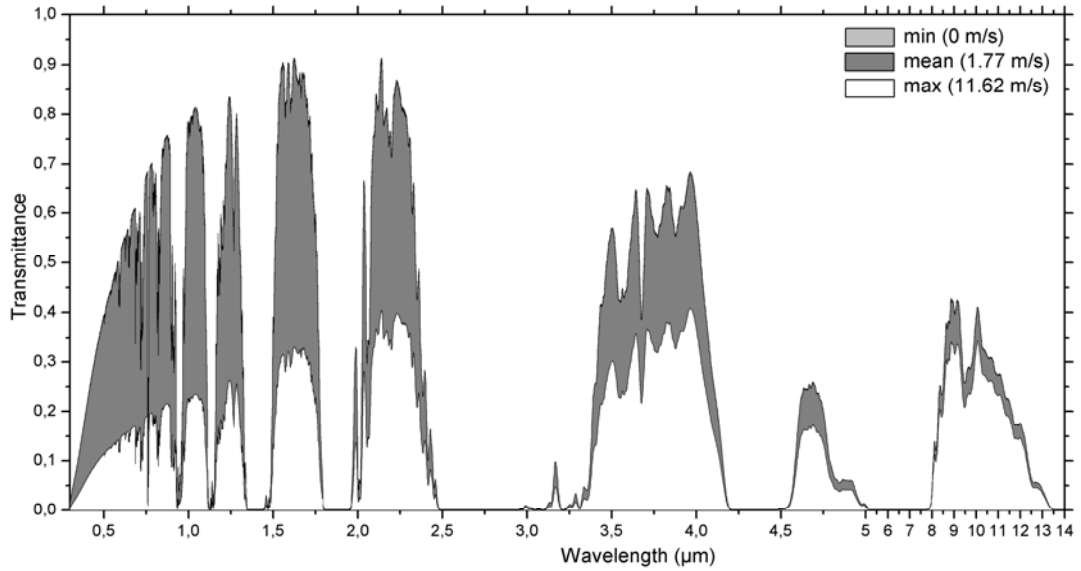

Figure 3.5. The effect of wind speed on atmospheric transmittance in winter season (December 2004 – February 2005) (0 m/s wind speed indicates calm atmosphere).

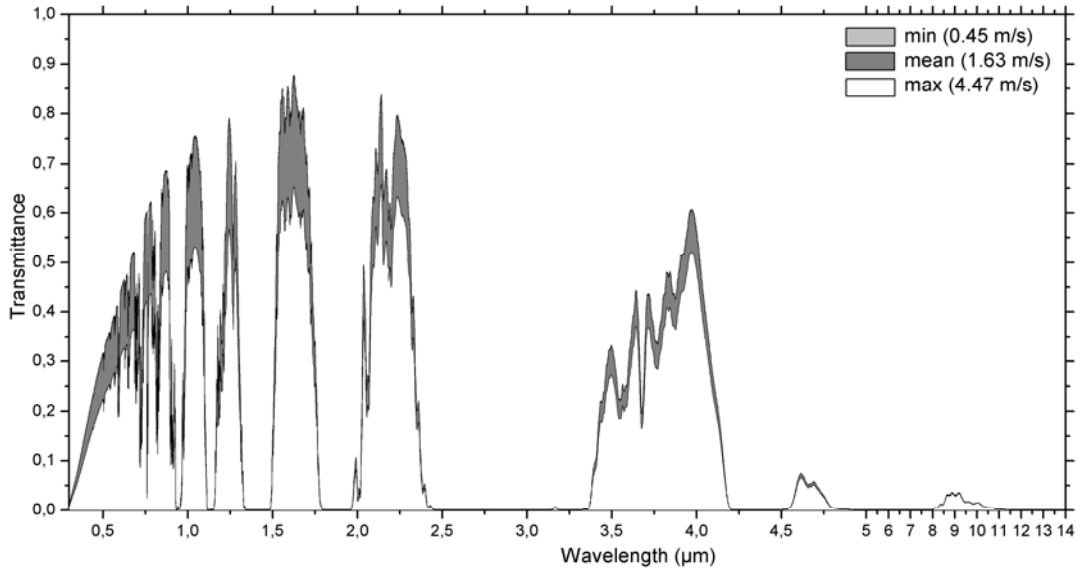

Figure 3.6. The effect of wind speed on atmospheric transmittance in summer season (June 2005 – August 2005).

As seen in Figure 3.7, atmospheric transmittances for minimum, mean and maximum pressure values are exactly the same. Furthermore, the calculations for summer season end up with the same AT. Therefore, AT for only winter season is given. The range of observed seasonal values of pressure is not enough to affect the AT.

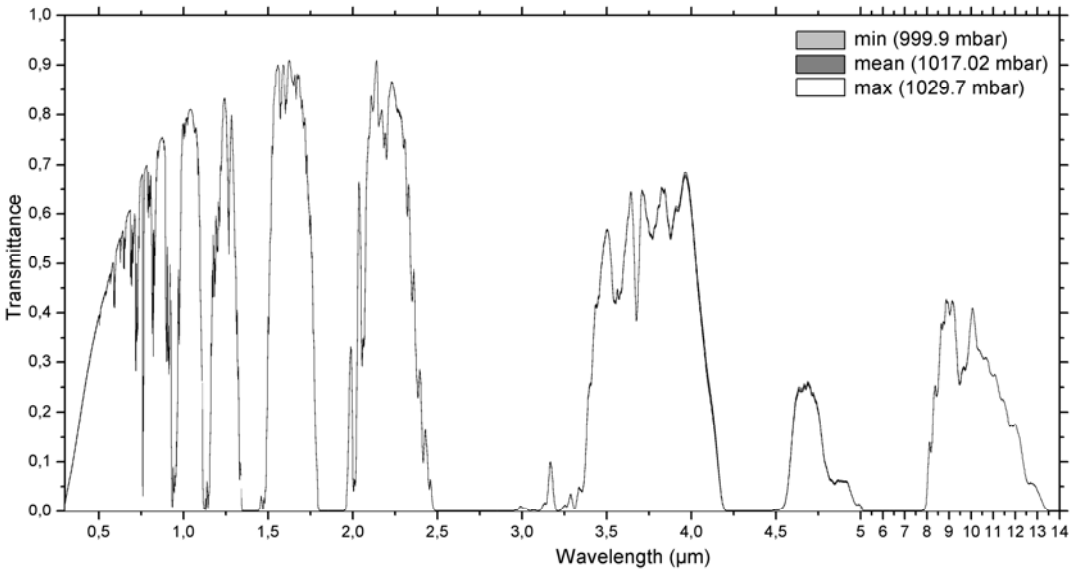

Figure 3.7. The effect of pressure on atmospheric transmittance in winter season (December 2004 – February 2005).

As seen in Figures 3.8 and 3.9, below 2.5 μm region, AT decreases with increasing air mass parameter. Since the sizes of continental aerosols have generally smaller than that of marine aerosols [33], effect of aerosol scattering and absorption due to continental aerosol component variations is strongly seen at smaller wavelengths.

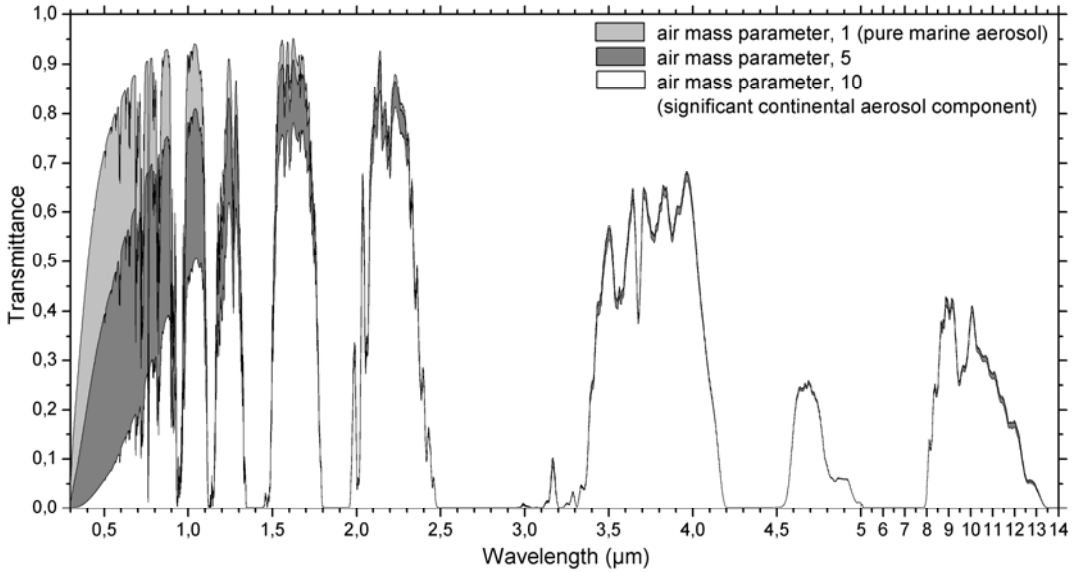

Figure 3.8. The effect of continental aerosols on seasonal averaged atmospheric transmittances in winter season (December 2004 – February 2005).

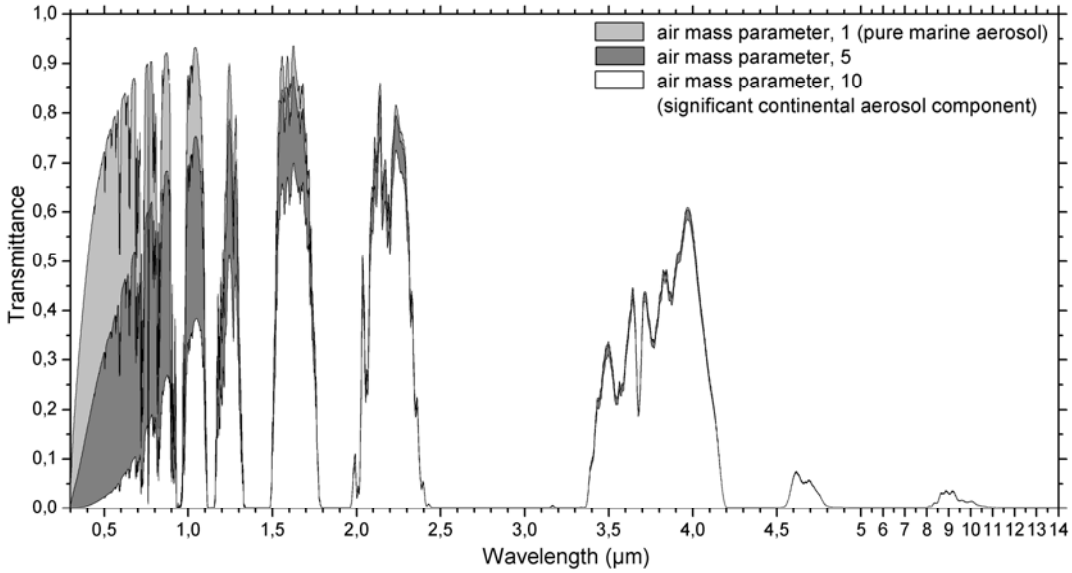

Figure 3.9. The effect of continental aerosols on seasonal averaged atmospheric transmittances in summer season (June 2005 – August 2005).

3.4. Determining the Desired Wavelength Interval(s)

The effect of a meteorological parameter on AT can be defined as,

$$\Delta T\left(\lambda\right)=\left|\,T_{\min}\left(\lambda\right)-T_{\max}\left(\lambda\right)\right| \tag{3.1}$$

where $T_{\min}\left(\lambda\right)$ and $T_{\max}\left(\lambda\right)$ are the AT's corresponding to minimum and maximum values of the meteorological parameter, respectively (see Figures 3.1 to 3.7). In order to define the wavelength(s) where the variations of AT due to the meteorological parameter is relatively low, and the AT is relatively high, an expression, $\phi\left(\lambda\right)$, can be defined as,

$$\phi\left(\lambda\right)=\frac{\Delta T\left(\lambda\right)}{T\left(\lambda\right)} \tag{3.2}$$

where $T\left(\lambda\right)$ is the seasonal average AT obtained by using seasonally arithmetic mean values of all meteorological parameters. If $\Delta T\left(\lambda\right)$ is low, and $T\left(\lambda\right)$ is high, then $\phi\left(\lambda\right)$ reaches to its minimum value. For the purpose of covering the effects of all meteorological parameters, since these meteorological parameters are coupled, the Equation 3.2 can be rewritten in the following form:

$$\phi\left(\lambda\right)=\sum_{i=1}^{4}\frac{\Delta T_i\left(\lambda\right)}{T\left(\lambda\right)}=\sum_{i=1}^{4}\frac{\left|\,T_{i,\min}\left(\lambda\right)-T_{i,\max}\left(\lambda\right)\right|}{T\left(\lambda\right)} \tag{3.3}$$

where i (i=1,2,3,4) denotes the meteorological parameters; pressure, temperature, relative humidity, and wind speed.

Values of $\phi\left(\lambda\right)$ are calculated by using MATLAB [34] mathematical tool. In order to eliminate low transmittance values, $\phi\left(\lambda\right)$ values are calculated by neglecting the $T\left(\lambda\right)$ values smaller than 0.01.

Calculated $\phi(\lambda)$'s are shown in Figure 3.10 for winter and summer seasons for air mass parameter of 5, and in Figures 3.11 and 3.12 for winter and summer seasons, respectively, for differing air mass parameters.

From the Figure 3.10, it is seen that, for both winter and summer seasons, $\phi(\lambda)$ takes its lower values in the wavelength region centered around 4 μm. For winter, lower values of all $\phi(\lambda)$'s are in the wavelength region centered around 4 μm (Figure 3.11); however, for summer, $\phi(\lambda)$ takes its lower values at around 1.6 μm for air mass parameter of 1, and around 4 μm for air mass parameter of 5 and 10 (Figure 3.12).

Considering all seasons and continental influence, it is evidently seen (Figures 3.10, 3.11, and 3.12) that lower values of $\phi(\lambda)$'s correspond to wavelength interval 3.99 μm to 4.02 μm (where the seasonal averaged AT's fall between $\mp$ 10% of AT's at wavelength that $\phi(\lambda)$ is evidently minimum).

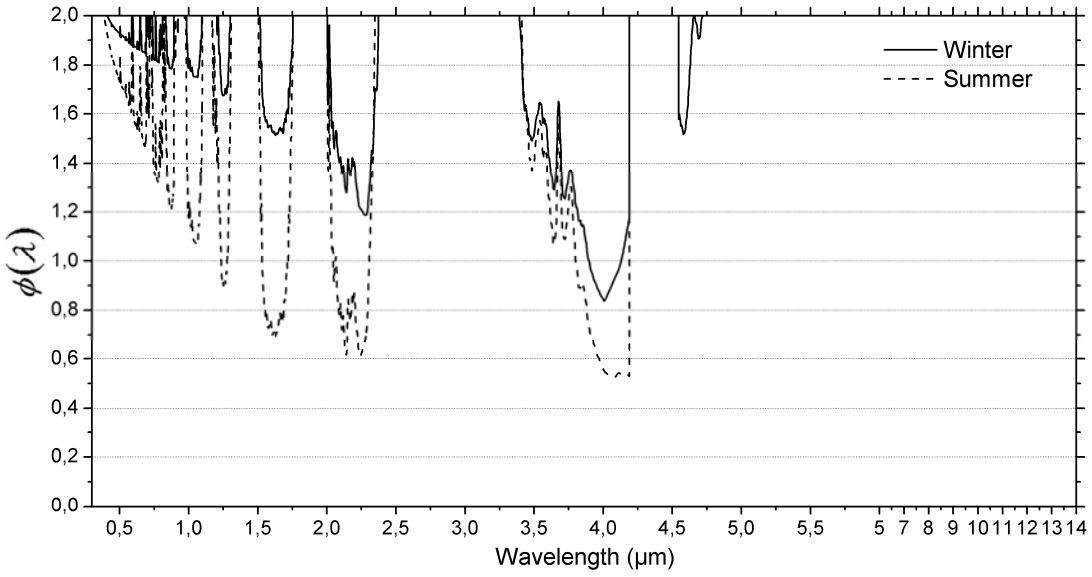

Figure 3.10. Calculated $\phi(\lambda)$'s for winter and summer seasons with air mass parameter of 5.

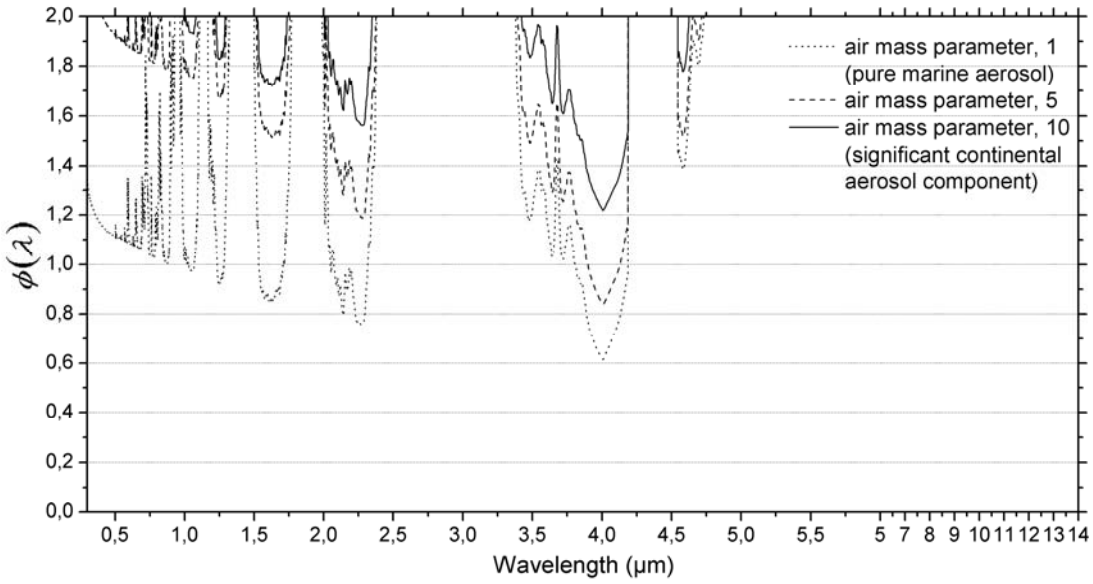

Figure 3.11. Calculated $\phi(\lambda)$'s for winter season with differing air mass parameters.

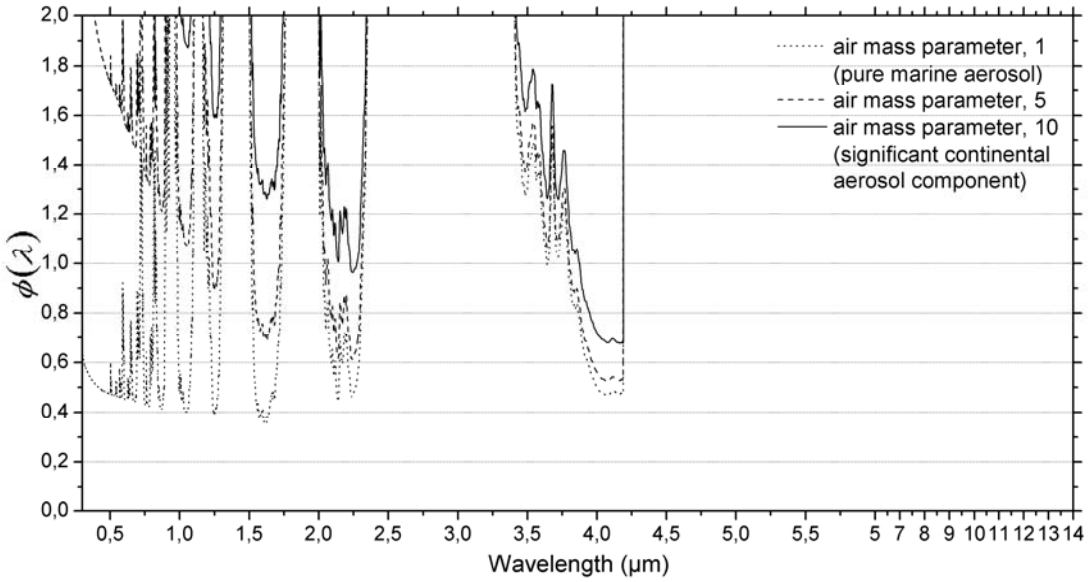

Figure 3.12. Calculated $\phi(\lambda)$'s for summer season with differing air mass parameters.

CHAPTER 4

CONCLUSION

In this work, effects of meteorological parameters (i.e. pressure, temperature, relative humidity, and wind speed) on atmospheric transmittance is studied in order to determine suitable wavelength interval(s) at which the atmospheric transmittance is high, and variation due to meteorological parameters is low. Alanya is selected for geographical location, and two seasons are covered (winter and summer). The laser propagation path is taken to be horizontally aligned to Earth's surface with an elevation of 10 m. The atmosphere including the propagation path is considered to be over sea surface, clean (i.e. includes no fog, rain, snow etc.) atmosphere. Continental influence of the sea surface atmosphere is also taken into account. Throughout the work, the spectral region of 0.3 μm to 1.4 μm is scanned.

It is determined that atmospheric transmittance is inversely proportional to three of the basic meteorological parameters, namely temperature, relative humidity and wind speed. It is shown that the pressure variations do not change the atmospheric transmittance considerably.

The effects of these parameters on atmospheric transmittance depend on wavelength. Temperature is determined to be strongly effective on atmospheric transmittance at wavelengths longer than 4.5 μm. The reason is that the absorption of water vapor molecule is much more influenced from temperature changes above 4.5 μm wavelength region. Below 2.5 μm, the effect of temperature is determined to

be negligible. In between 3 μm and 4.5 μm region, variations of atmospheric transmittance are much less than that of above 4.5 μm.

Unlike temperature, it is determined that the relative humidity is effective on AT over a spread of wavelengths (i.e. 0.3-14 μm). The main reason of decrease in AT due to relative humidity, arise from scattering and absorption by aerosols. Condensation of water vapor onto aerosols yields serious variations on AT. Below 2.5 μm region, AT is more influenced by relative humidity. As the wavelength decreases, the fluctuations of atmospheric transmittance increase. Additionally, above 4.5 μm, the water vapor absorption is more influenced from relative humidity changes.

The wind speed is determined to be permanently effective at the entire spectral region (i.e. 0.3-14 μm). As similarly to the relative humidity variations, the wind speed is also strongly effective below 2.5 μm region. The effect of wind speed is due to increase in marine aerosol population yielding substantial increase in aerosol scattering and absorption.

The influence of sea surface atmosphere by continental aerosols is determined to be affecting the atmospheric transmittance below 2.5 μm region. Atmospheric transmittance is inversely proportional to the continental influence. Additionally, for wavelength region below 2.5 μm, as the wavelength decreases, variations in atmospheric transmittance increase due to the continental influence. Since the sizes of continental aerosols are generally smaller than that of marine aerosols, the aerosol scattering and absorption effect due to continental aerosol variations is strongly seen at smaller wavelengths.

In the case of considering all the effects of meteorological parameters, for both summer and winter seasons, and considering a wide range of continentally influenced atmosphere, the wavelength interval at which the atmospheric transmittance variations being relatively low and transmittance being relatively high is found to be about between 3.99 μm and 4.02 μm.

There is an evident lack of information about the atmospheric constituents in Turkey. It is important that the concentrations of important gases and aerosols should be measured periodically, like other countries do. In the further study, this introductory work can be extended to other geographical locations in Turkey with extensive collection of information about atmospheric composition.

REFERENCES

1. Encyclopedia of Laser Physics and Technology, *http://www.rp-photonics.com/optical_data_transmission.html*, [last accessed date: 30 August 2006].
2. Manor H., Arnon S., *Performance of an optical wireless communication system as a function of wavelength*, Optical Society of America, 2003.
3. Leitgeb E., Muhammad S.S., Chlestil C., Gebhart M., Binrbacher U., *Reliability of FSO Links in Next Generation Optical Networks*, IEEE, 2005.
4. Smith F.G., *The Infrared & Electro-Optical Systems Handbook, Volume 2, Atmospheric Propagation of Radiation*, SPIE Optical Engineering Press, 1993.
5. Kopeika N.S., *General wavelength dependence of imaging through the atmosphere*, Applied Optics 20, 1532–1536, 1981.
6. NOAA Satellite and Information Service, National Climatic Data Center (NCDC) Website, *http://www.ncdc.noaa.gov/oa/ncdc.html*, [last accessed date: 22 August 2006].
7. Goody R.M., Yung Y.L., *Atmospheric Radiation Theoretical Basis*, Second Edition, Oxford University Press, 1989.
8. Ricklin J.C., Hammel S.M., Eaton F.D., Lachinova S.L., *Atmospheric Channel Effects on Free-Space Laser Communication, Springer Science*, J. Opt. Fiber. Commun. Rep. 3, 111-158, 2006.
9. Kneisys, F.X., Abreu, L.W., Anderson G.P., Chetwynd J.H., Shettle E.P., Berk A., Bernstein L.S., Robertson D.C., Acharya P., Rothman L.S., Selby J.E.A., Gallery W.O., Clough S.A., *The MODTRAN 2/3 and LOWTRAN 7 Model*, Phillips Laboratory, Geophysics Directorate, 1995.
10. Bass M., *Handbook of Optics, Volume I*, Second Edition, Optical Society Of America, 1995.

11. Weichel H., *Laser Beam Propagation in the Atmosphere*, SPIE Optical Engineering Pres, 1990.
12. *Liou K.N., An Introduction to Atmospheric Radiation*, Second Edition, Academic Press, *2002.*
13. NOAA Jetstream Website, *http://www.srh.noaa.gov/srh/jetstream/atmos/atmos_intro.htm*, [last accessed date: 1 September 2006].
14. Wikipedia Website, *http://en.wikipedia.org/wiki/Earth%27s_atmosphere*, [last accessed date: 1 September 2006].
15. Wikipedia Website, *http://en.wikipedia.org/wiki/Karman_line*, [last accessed date: 1 September 2006].
16. NOAA Jetstream Website, *http://www.srh.noaa.gov/srh/jetstream/atmos/layers.htm*, [last accessed date: 1 September 2006].
17. Anderson G.P., Clough S.A., Kneizys F.X., Chetwynd J.H., Shettle E.P., *AFGL Atmospheric Constituent Profiles (0-120km),* Air Force Geophysics Laboratory (AFGL), 1986.
18. Vision Learning Website, *http://www.visionlearning.com/library/module_viewer.php?mid=107&l=&c3=*, [last accessed date: 1 September 2006].
19. *http://www.windows.ucar.edu/tour/link=/earth/Atmosphere/layers.html*, [last accessed date: 1 September 2006].
20. NOAA Jetstream Website, *http://www.srh.noaa.gov/srh/jetstream/atmos/ionosphere_max.htm*, [last accessed date: 1 September 2006].
21. Dogan G., *Comparison of the Rural Atmosphere Aerosol Compositions at Different Parts of Turkey*, Ms Thesis, Middle East Technical University, 2005.

22. Lide D.R., *CRC Handbook of Chemistry and Physics*, 87th Edition, CRC Pres, 2006-2007.
23. Rothman L.S., Jacquemart D., Barbe A., Benner D.C., Birk M., *The HITRAN 2004 molecular spectroscopic database*, Elsevier, 2005.
24. HITRAN Website, *http://cfa-www.harvard.edu/HITRAN/*, [last accessed date: 1 September 2006].
25. Kopeika N.S., Bordogna J., *Background Noise in Optical Communication Systems*, Proceedıngs Of The IEEE, Vol. 58, No. 10, 1970.
26. RJH A.R., *Infrared Technology Applications to Electrooptics, Photonic Devices, and Sensors*, John Wiley & Sons, 2000.
27. Bohren C.F., Bass M., *Handbook of Optics, Volume I*, Second Edition, Chapter 6, Optical Society Of America, 1995.
28. Hahn D.W., *Light Scattering Theory*, Department of Mechanical and Aerospace Engineering University of Florida, 2004.
29. Driggers, R.G., Cox P., Edwards, T., *Introduction to Infrared and Electro-Optical Systems*, Artech House, 1999.
30. MieCalc - freely configurable program for light scattering calculations (Mie theory) Website, *http://www.lightscattering.de/MieCalc/eindex.html*, [last accessed date: 1 September 2006].
31. Zeisse C.R., *NAM6: Batch Code for the Navy Aerosol Model*, Technical Report, SSc San Diago, 1999.
32. World Data Centre for Greenhouse Gases (WDCGG) Website, *http://gaw.kishou.go.jp/wdcgg.html*, [last accessed date: 22 August 2006].
33. Gathman S.G., *The Aerosol of the Marine Environment*, Proceedings of SPIE, Vol. 3927, 2000.
34. MathWorks Website, *http://www.mathworks.com/*, [last accessed date: 4 September 2006].

35. IRI/LDEO Climate Data Library Website, *http://ingrid.ldeo.columbia.edu/dochelp/QA/Basic/dewpoint.html*, [last accessed date: 1 September 2006].

36. The Air Force Research Lab, Space Vehicles Directorate, *http://www.vs.afrl.af.mil/ProductLines/IR-Clutter/modtran4.aspx*, [last accessed date: 1 September 2006].

37. Ontar Corporation, 2004, *PcModWin Manual Version 4.0 v3r1 Version 1.2*, 9 Village Way, North Andover, MA 01845, USA.

APPENDIX A

RELATIVE HUMIDITY

Relative humidity is a unit to quantify the amount of water vapor (H_2O) rather than pressure units [4]. It is the ratio of how much moisture the air is holding to how much moisture it could hold at a given temperature [35]. It can be expressed as the ratio of H_2O partial pressure, pH_2O, to the saturation vapor pressure, $E_s(T)$ [4]:

$$RH = \left[\frac{pH_2O}{E_s(T)} \right] \times 100\% \tag{A.1}$$

where $E_s(T)$ is in units of kilo-pascals (kPa) (1atm = 1013 mbar = 101.3 kPa = 760 torr). Saturation vapor pressure can be computed by the following formula with an accuracy of 0.1% [4]:

$$E_s(T) = 2.4096 \left(\frac{300}{T} \right)^5 10^{(10-2950.2/T)} \text{ (kPa)} \tag{A.2}$$

where T is temperature in Kelvin.

APPENDIX B

MODTRAN (MODERATE RESOLUTION TRANSMITTANCE CODE)

MODTRAN [9] is one of the widely used computer codes in order to calculate atmospheric transmittance and radiance using complex detailed algorithms. MODTRAN is developed over the past 25 years at the US Air Force Research Laboratory, formerly Air Force Geophysics Laboratory (AFGL), at Hanscom AFB, MA [36].

Its calculations covers frequencies from 0 to 50,000 cm^{-1} at moderate spectral resolution; 2 cm^{-1} resolution from 0 to 22.680 cm-1 (440 nm), and 20 cm^{-1} resolution between 22.680-50.000 cm^{-1} (200-440 nm) [36].

For molecular absorption calculations, MODTRAN uses a two-parameter equivalent width band model (proportional to temperature and pressure) that employs large pre-stored spectral data bases. The data bases are derived directly from the spectral line parameters on the HITRAN [23] data base (see section 2.4.2) for each molecular species, plus cross sections for the heavy molecules (e.g. Chlorofluorocarbons). For local thermodynamic equilibrium conditions only, temperature ranges are 180 K – 320 K. Molecular scattering (Rayleigh scattering), and Aerosol scattering and absorption (Mie Theory) are included for transmittance and radiance calculations [36].

The atmosphere is treated as plane parallel, sliced into 33 atmospheric layers, from 0 to 100 km altitude. Physical parameters, such as pressure, temperature, molecular absorption, and extinction coefficients are defined for each layer [37].

Six AFGL standard atmosphere models [17] (see Section 2.1.3) are included, or the user can provide a custom atmospheric profile based on direct measurements or radiosonde profiles. For aerosol/particle optical properties, a wide range of standard aerosol models (see Section 2.1.5), or user-supplied ones can be used [37].